SCHOLAR COMMONS
USF UNIVERSITY OF SOUTH FLORIDA

University of South Florida
Scholar Commons

Graduate Theses and Dissertations | Graduate School

January 2013

Reliability Assessment of Ion Contamination Residues on Printed Circuit Board

Minh Tam Tran Nguyen
University of South Florida, mtnguye9@mail.usf.edu

Follow this and additional works at: http://scholarcommons.usf.edu/etd

Part of the Mechanical Engineering Commons

Scholar Commons Citation
Nguyen, Minh Tam Tran, "Reliability Assessment of Ion Contamination Residues on Printed Circuit Board" (2013). *Graduate Theses and Dissertations.*
http://scholarcommons.usf.edu/etd/4551

This Thesis is brought to you for free and open access by the Graduate School at Scholar Commons. It has been accepted for inclusion in Graduate Theses and Dissertations by an authorized administrator of Scholar Commons. For more information, please contact scholarcommons@usf.edu.

المنارة للاستشارات
www.manaraa.com

Reliability Assessment of Ion Contamination Residues on Printed Circuit Board

by

Minh Tam Tran Nguyen

A thesis submitted in partial fulfillment
of the requirements for the degree of
Master of Science in Mechanical Engineering
Department of Mechanical Engineering
College of Engineering
University of South Florida

Co-Major Professor: Ashok Kumar, Ph.D.
Co-Major Professor: Kantesh Doss, Ph.D.
Rasim Guldiken, Ph.D.
Manoj K. Ram, Ph.D.
Craig Lusk, Ph.D.

Date of Approval:
March 22, 2013

Keywords: Ion Chromatography, Water Drop Test, Electrochemical Migration, Soldering Process, Time to Failure

Copyright © 2013, Minh Tam Tran Nguyen

www.manaraa.com

DEDICATION

To my parents, brothers, and sisters

المنارة للاستشارات

www.manaraa.com

ACKNOWLEDGMENTS

I'd like to express my deepest gratitude to my co-major advisor Dr. Ashok Kumar, co-major advisor Dr. Kantesh Doss, for their tremendous support and guidance.

I'd like to extend this gratitude to Mr. Art Rawers, Mr. Arnold Hogrefe, Ms. Shannon Tefft and everyone at Jabil's Advanced Manufacturing Technology for their encouragement. I'd like to thank Dr. Rasim Guldiken, and Dr. Craig Lusk and Dr. Manoj Ram for their time, effort, and advice as committee members.

I'm greatly thankful to my colleagues at USF's Advanced Materials Research Lab for their assistance.

This work would have never been completed without all of you.

المنارة للاستشارات

www.manaraa.com

TABLE OF CONTENTS

LIST OF TABLES iii

LIST OF FIGURES iv

ABSTRACT vii

CHAPTER 1: INTRODUCTION 1

CHAPTER 2: BACKGROUND AND LITERATURE REVIEW 3
- 2.1 Printed Circuit Board 4
- 2.2 Metals 6
- 2.3 Flux 7
- 2.4 Assembly Soldering Process 9
  - 2.4.1 Solder Joint 9
  - 2.4.2 Fundamental of Soldering 10
  - 2.4.3 Soldering Mechanism 11

CHAPTER 3: ELECTROCHEMICAL MIGRATION 13
- 3.1 ECM Definition 13
- 3.2 ECM Mechanisms 13
- 3.3 ECM Drivers 16
  - 3.3.1 Voltage and Electric Field 16
  - 3.3.2 Contamination 16
  - 3.3.3 Time to Failure Models 17
    - 3.3.3.1 Arrhenius Model 17
    - 3.3.3.2 Baron and Bockris 18

CHAPTER 4: EXPERIMENTAL METHODS 20
- 4.1 Characterization Technique 20
  - 4.1.1 Cross-Sectioning 20
  - 4.1.2 Ion Chromatography 23
    - 4.1.2.1 Ion Chromatography Preparation 26
      - 4.1.2.1.1 Localized Extraction 26
      - 4.1.2.1.2 Bag Extraction 28
- 4.2 Test Vehicle Design 28
- 4.3 Water Drop Test Procedure and Setup 32
- 4.4 Design of Experiment 35
- 4.5 Cleaning Process 36

المنارة للاستشارات
www.manaraa.com

4.6 Water Drop Test 37

CHAPTER 5: RESULTS 40
5.1 Cleaning Process Result 40
5.2 DOE Parameter Selection 41
5.2.1 Succinate Effectiveness Result 41
5.2.2 Final DOE Matrix 41
5.3 DOE Test Result 42
5.4 Effect of Pad Geometry and Field Strength on ECM Susceptibility 45
5.5 Interaction Between Factors 48
5.6 Statistical Analysis 50

CHAPTER 6: CONCLUSION AND FUTURE WORK 54
6.1 Conclusion 54
6.2 Future Work 54

REFERENCES 57

APPENDICES 60
Appendix A: Collected Data for Ion Chromatography 61
Appendix B: Collected Data for Conductivity Test 68
Appendix C: Permission Release for Use of Result from Work at Jabil Inc. 69

www.manaraa.com

LIST OF TABLES

Table 1: Typical rosin composition 8

Table 2: Soldering mechanism 11

Table 3: Test vehicle PCB design parameters and variables 29

Table 4: Test PCB pad design 30

Table 5: Test cell materials 31

Table 6: DOE parameter matrix 36

Table 7: DOE matrix for concentration 38

Table 8: Final DOE matrix 42

Table 9: DOE result 42

المنارة للاستشارات

www.manaraa.com

LIST OF FIGURES

Figure 1: Cross section of multilayers board 4

Figure 2: Electronic packaging technology 5

Figure 3: Formation of tin-lead dendrite 6

Figure 4: PCB manufacturing process chart 8

Figure 5: Steps in solder joint formation 10

Figure 6: Interrmetallic formation 10

Figure 7: Electrochemistry of ECM 14

Figure 8: Ionic migration 14

Figure 9: Example of a sample mounting mold 20

Figure 10: Illustration of epoxy being poured into the mounting cup/mold 21

Figure 11: The images (from left to right) of the target areas at 320 and 400 grit papers 22

Figure 12: The images (from left to right) of the target areas at 600, 800, and 1200 grit papers 22

Figure 13: The images (from left to right) of the target areas after polishing at 3.0, 1.0. and 0.5 micron colloidal silica suspension 22

Figure 14: Schematic diagram showing the ion exchange process 23

Figure 15: Ion chromatography data from an anion analysis of glacial water 25

Figure 16: Ion chromatography 25

Figure 17: C3 cleanliness tester-localized extraction 26

Figure 18: C3 cleanliness test cell 27

المنارة للاستشارات

www.manaraa.com

Figure 19: Bag extraction process 28

Figure 20: The cross-sectioning of test cell structure 30

Figure 21: Fabricated lead free cell 31

Figure 22: Fabricated tin-lead cell 31

Figure 23: Completed fabricated test vehicle layout 32

Figure 24: Water drop test equipment set up: (1) power supplier-lambda LLS8040, (2) keithley picoammeter, (3) pipetter, (4) anion samples 32

Figure 25: Water drop test equipments set up: (5) CRT monitor, (6) computer screen (with excel data display) 33

Figure 26: Water drop test equipments set up: (7) microscope, (8) test vehicle board, (9) gator connector cable 33

Figure 27: Flow chart illustrating set up procedure 35

Figure 28: Cleaning process flow chart 37

Figure 29: Electrochemical migration of Br- on tin-lead board: (a) virgin board, (b) ECM growth, (c) ECM bridge 38

Figure 30: Electrochemical migration of Br- on lead free board: (a) virgin board, (b) ECM growth, (c) ECM bridge 39

Figure 31: Ion chromatography anions results 40

Figure 32: ECM plot (Current vs. Time) for 1000ppm succinate ions on tin-lead (Sn-Pb) and lead free (Pb free) boards 41

Figure 33: ECM plot (Current vs. Time) for 3 ppm Chloride anion on tin- lead 12.5 mils spacing 44

Figure 34: ECM plot (Current vs. Time) for 3 ppm Cl^- on tin lead_25.0 mils spacing 45

Figure 35: Aspect ratio vs. time 46

Figure 36: Current and spacing on tin lead board 46

Figure 37: Time to failure vs. spacing on tin lead board 47

المنارة للاستشارات
www.manaraa.com

Figure 38: Current vs. spacing on lead free board........47

Figure 39: Time to failure vs. spacing on lead free board........48

Figure 40: Interaction plot of factors for time (sec)........49

Figure 41: Interaction plot of factors for current (milliamps)........49

Figure 42: Data analysis of variances on time to failure........50

Figure 43: Data analysis of variances on current........51

Figure 44: Variables vs. time to failure (sec)........51

Figure 45: Variables vs. current at failure (milliamps)........52

Figure 46: Total anions (ppm) over WDT current vs. test variables........52

Figure 47: Ppm over time vs. test variables........53

Figure 48: Gold nanoparticles under TEM x 20 nm........55

Figure 49: Potential vs. current density of Zn^{2+} in gold nanoparticles solution........56

المنارة للاستشارات

www.manaraa.com

ABSTRACT

Ion contaminants from Printed Circuit Board (PCB) assembly processes pose a high reliability risk because they result in damaged circuits. Therefore, it is essential to understand the level of ionic species on the electronic circuitry as well as the reliability risks caused by these contaminants. There are a number of approaches available in the industry to assess the reliability risks ; for example, the water drop test (WDT) is one of the techniques used to determine the propensity of an ionic contaminant to cause electrical short failures by dendrite formation. The objective of this research is to determine the time to cause the failures, known as electrochemical migration (ECM) failures. A test vehicle was developed for the WDT to obtain the time to cause ECM failure in presence of different anions. The time to form dendritic bridges that cause short circuits was determined as a function of the different anions and the spacings between PCB pads. The experimental method involved dispensing aqueous solutions containing common inorganic and organic acid anions onto test vehicles, applying electrical bias voltages and measuring the time to form dendrites. Specially designed test structures cells were created to contain the test solutions. At each of the test cells, a cavity held the solution and constant current was applied through different metal geometries. To be representative of popular board finishes, test vehicle boards incorporated both Sn-Pb Hot Air Soldering Level (HASL) and Pb free HASL surface finishes.

المنارة للاستشارات
www.manaraa.com

CHAPTER 1: INTRODUCTION

The trend towards electronic component densification and miniaturization demands a steadily decreasing PCB pad spacing (Harsanyi, 1995) (D.Q. Yu et al, 2006) in Surface Mount Technology (SMT) assemblies. In order for these assembly systems to continue to work reliably in the field, they must survive an environment with heat, moisture and electrical bias. It is observed that the occurrence of resistive shorts in the electronic circuitry that cause field failures varies under different physical, chemical, electrical, environmental and electrochemical and design conditions. One of the phenomena that cause shorts in electronic circuits on the PCB assemblies is electrochemical migration (ECM). This can be defined as a movement of metal ion through an electrolytic solution under an applied electric field between adjacent conductors (Harsanyi, 1995). ECM occurs on or in almost all electronic packages and assemblies via dendritic growth. Ultimately, dendrite growth reduces the gap between two adjacent metal stripes that leads to the current leakage and intermittent shorts and consequently increases the chance of catastrophic failure (Noh et al, 2008).

A number of reports have been published about the methods for investigating the ECM behavior of a sample (O. Devos, C. Gabrielli, L. Beitone, C. Mace, E. Ostermann, H. Perrot, 2007), (W. Jud Ready, Laura J. Turbini, Roger Nickel, and John Fischer, 1999), (Harsanyi, 1995). Furthermore, much research has been done in comparing and testing the effectiveness of cleaning systems for post soldered PCBA such as ROSE,

المنارة للاستشارات
www.manaraa.com

C3/IC and SIR (Kong Hui Lee, Rob Jukna, Jim Altpeter, Kantesh Doss, 2011), (Pravin Sequeira et al, 2010). The most common test method employed to study ECM is the water drop test which is performed by dispensing a drop of deionized water between adjacent PCB pads or traces (IPC TM650, 2.6.1) and applying an electrical bias.

It is a challenge to achieve repeatable results in water drop test if it is performed on typical PCBs owing to interference from other lines and traces and the inability to maintain consistent volume of the water. The first step in this study was to design and fabricate a test vehicle with known cell geometry. The second step is to determine the value of concentrations of anions that would cause ECM short. Ultimately, the goal for this study was to determine the time to electrochemical failures by ECM for known conductor spacing, anion concentrations.

المنارة للاستشارات
www.manaraa.com

CHAPTER 2: BACKGROUND AND LITERATURE REVIEW

Electronic equipment is a combination of electronic components connected electrically to produce a certain designed function. In the early days of electronic industry, electronic equipment were constructed by soldering and hand wiring. Therefore, the equipment was bulky, large, awkward, and unlikely to meet the demands of small equipment required in aerospace, health sector, and home's applications.

A natural evolution took place in many fields in around 1950s (Stearns, 1996). To decrease the time between unit failure and repair due to easy replaceability, the smaller components were developed. The use of miniaturization in electronic equipment design created a new technology that is popular known as the printed circuit board.

There are many advantages in using a PCB instead of other interconnection and mounting techniques. The most important reason is that the size of component assembly is reduced with corresponding decrease in weight. Thus, a higher quantity of production can be achieved at lower cost. Besides, PCBs also ensure a high level of repeatability, offer uniformity of electrical characteristic, and eliminate the probability of manufacturing errors (Strauss, 1994).

On the other hand, the miniaturization creates several issues. One of the problems is the electrochemical migration on components that leads to short in the electronic circuitry. (Harsanyi, 1995). Furthermore, the boards can be contaminated easily while be handled (Hymes, 1991).

المنارة للاستشارات
www.manaraa.com

There are many variables that make it difficult to understand the specifies nature of the electrochemical failure mode. However, five majors factors are the construction of printed circuit boards, the metals used in the board assemblies, process materials such as flux and its removal, the soldering process and electrochemistry.

2.1 Printed Circuit Board

Printed circuit boards are formed by a thin layer of conducting material (e.g. Cu) deposited, or "printed," on the surface of an insulating board known as the substrate. Four different PCB constructions are single side, double side, multilayer, and flexible boards. Single side boards have components only on one side of the laminate material. When more components are required, double side is used. In the third type, multilayer boards, the components are mounted on both sides of the insulating material with additional conductor layers in between the top and bottom layers. Typical constructions vary between three and as high as thirty-two layers.

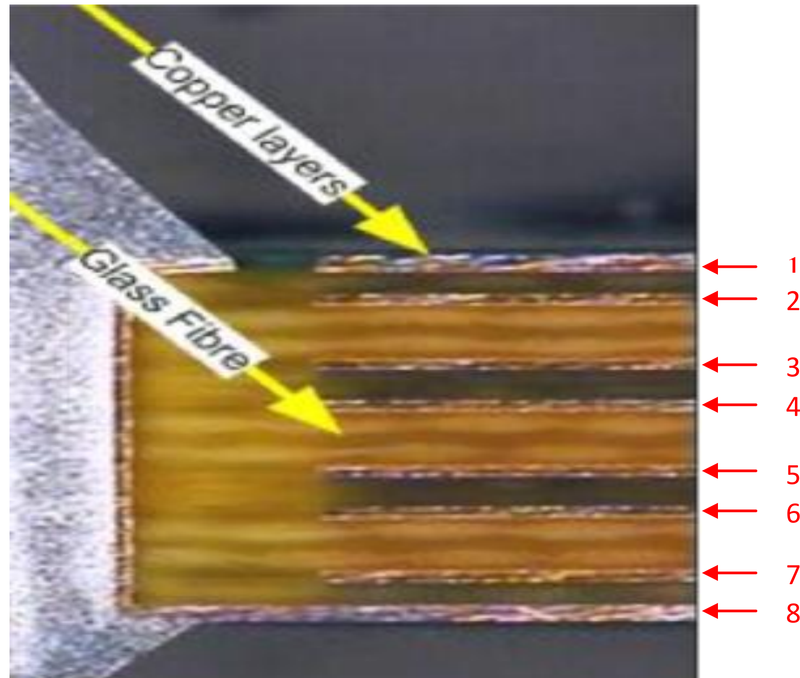

Figure 1: Cross section of multilayers board (Lawson, 2007)

www.manaraa.com

Figure 1 presents a cross section of multi-layer board showing alternate layers of copper and dielectric layers (FR4 laminate). The final type, the flexible board is normally made up of three-layers of material: a base dielectric layer, a central conductor layer and top dielectric layer (Stearns, 1996). These are typically used in digital cameras, medical field or application where high density is required.

To connect components on the PCB, new packaging technologies have been developed. There are four popular technologies (figure 2) to attach components to the boards: plated through-hole (PTH), leaded SMT, leadless SMT, and ball grid array (BGA) (Capillo, 1990). PTH is the use of leads that are inserted into the hole drilled in PCB to mount the components. Leaded SMT is the method of soldering leaded components to the metalized pads on the PCBs. While leadless SMT is to mount non leaded SMT parts to the PCB's surface. (Deckert, 1987). On the other hand, BGA assembly is made up of balls in grid pattern to conduct electrical signal from PCB on which it's placed. This techniques is the most popular because of easy handling, robust, and compatibility with existing surface mount equipment (Capillo, 1990) (Deckert, 1987).

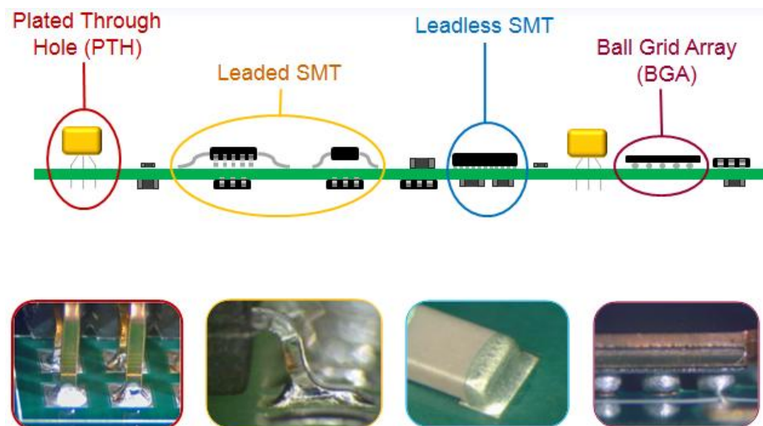

Figure 2: Electronic packaging technology (Doss, 2011)

المنارة للاستشارات
www.manaraa.com

2.2 Metals

In the electronics packaging manufacture, copper, tin and nickel are the most important metals for interconnection systems. Copper constitutes the main interconnection material used for PCB pattern while tin, nickel or nickel-based alloys and gold are used for other contact metallization that specifically prevent degradation or oxidation of copper during soldering process . These metals are involved in the ECM failure because of the formation of dendrites (figure 3), and subsequently current leakages and electrical shorts.

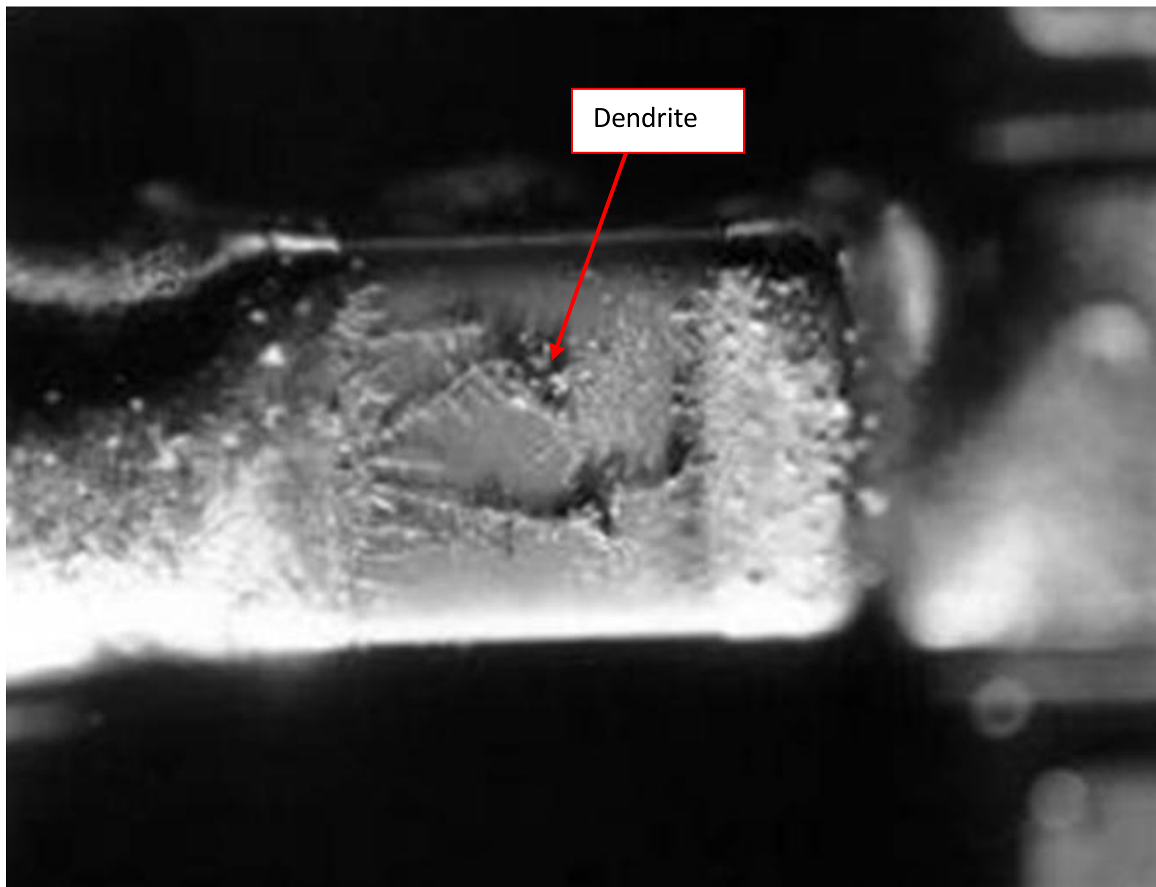

Figure 3: Formation of tin-lead dendrite (Delhi 2005)

Copper is replacing the nickel/iron alloy lead-frames and aluminum soldering joint. due to its better thermal conductivity and superior electrical conductivity (Murarka

المنارة للاستشارات
www.manaraa.com

Shyam P., Verner Igor V., and Gutmann Ronald J., 2000). However, using copper for soldering results in a higher risk of contamination due to a greater electrochemical migration susceptibility than its aluminum predecessor (Harsanyi, 1999)

When applying voltages to a PCB , under harsh environments such as high humidity , metal components tend to migrate electrochemically in ion forms and eventually lead to short circuit failures (Harsanyi G. , 1995) (Ready, W. J and Turnini, L. J., 2002) (Hwang, 1992).

2.3 Flux

Flux acts as a means for suspending the solder particles in the solder paste process. It imparts proper viscosity to the paste and also controls paste spreading after the print. Besides, it enables wetting of the metal surface to be soldered by removing the oxides and other surface films and reducing surface tension. Most importantly, it protects the surfaces of the exposed metal from the re-oxidizing at elevated temperatures. There are different types of fluxes in PCB assembly industry: rosin based flux, water soluble flux, and "no-clean" flux.

Rosin based flux consists of gelling or suspension agents, activators, solvents, thixotropic agents, and special additives. The percent of each constituents will decide the effectiveness of flux in general. Thus flux is designed for each application and normally contains up to 60% by weight of rosin, 7-10% thickeners, 5-10% viscosity agents and up to 2% activators (Lawson, 2007). To help flux perform better, variety of solvent such as alcohols (isopropyl, butyl alcohol and polyethylene glycol) are added to form the solution. Rosin is a major element in flux and natural chemical mixture extracted from pine trees. Table 1 shows the typical concentrations of several rosin acids.

المنارة للاستشارات
www.manaraa.com

Table 1: Typical rosin composition (Lawson, 2007) (Muren, 1994) (Hwang, 1992)

Rosin Acid	% Composition
Levopiramic	Trace
Neoabietic	10-20
Abietic	30-40
Isodextropimaric	8
Dextropinamirc	8
Dehydroabietic	5
Dihydroabietic	16
Tetra-abietic	16

Water soluble flux consists of highly active and corrosive organic acids. The PCB assembly process leaves behind significant level of corrosive flux residues on the board. Depending on the chemistry of the flux, the amount of flux and the geometry of boards and component, flux removal is a challenge for manufacturing operation because any flux left over on the board can accelerate the failure due to ECM. Therefore flux removal process is very important as indicated in the flow chart in figure 4.Typically, the water soluble flux residues are removed by an inline or a batch wash system that use DI water.

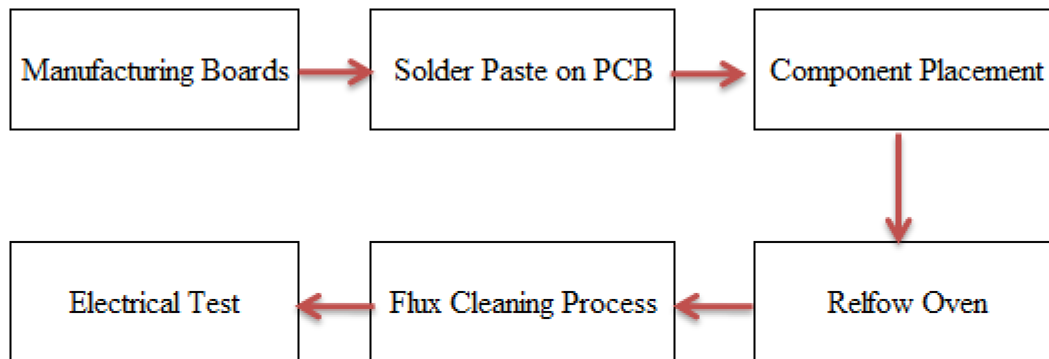

Figure 4: PCB manufacturing process chart

In the electronics industry, it's typical that the flux residues are cleaned after the PCB goes through the reflow soldering process employing water soluble pastes and

المنارة للاستشارات
www.manaraa.com

fluxes. High pressure deionized water solution provide the safest means of cleaning (Ellis, 1986). However, contamination after cleaning still occurs if the cleaning process is not strictly controlled.

"No clean" flux is used to eliminate the cost of water-based cleaning processes. However, it has been reported (Shangguan D., Achari A. and Green W., 1994) that dendrites can occur if no clean flux residues are left behind on electrically-biased. Thus, it is important that no "no clean" flux residues are left on the board. Any attempt to clean no clean flux residues using isopropyl alcohol or water can result in high level of ion contaminants which could lead to ECM failures.

2.4 Assembly Soldering Process

In the surface mount assembly operation, PCB soldering process is considered the most critical process that has the biggest effect on the electrochemical migration. In this regard, it is important to understand the fundamentals of soldering.

2.4.1 Solder Joint

Solder joint is a metallurgical connection formed between two different metal surfaces by melting and flowing a solder alloy having a lower melting point than the joint members themselves.

Solder joints carry electrical, mechanical and/or thermal loads. Electrically, they carry electric current across various circuits to various levels. Mechanically, they withstand the stresses of expansion and contraction as electronics heat up and cool down, and shock and vibration if they move or fall. Thermally, they draw heat away from processor chips and other components that run hot. Figure 5 is a flow chart showing various phases of solder joint formation.

المنارة للاستشارات
www.manaraa.com

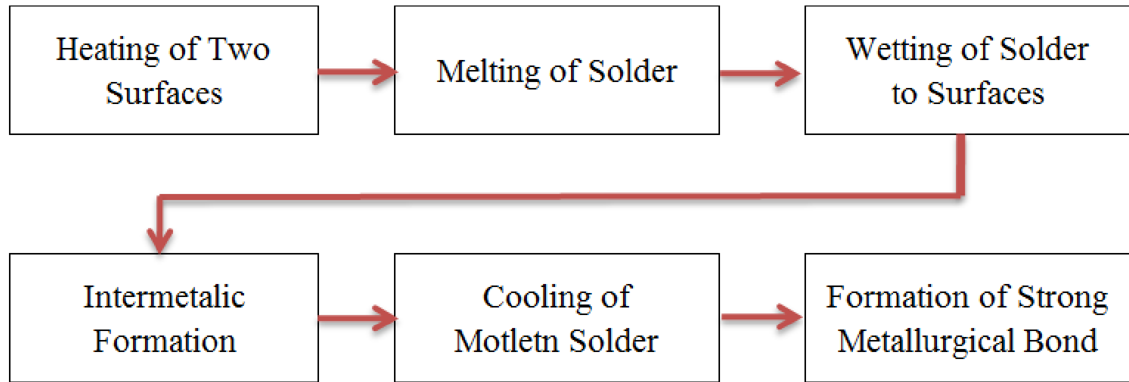

Figure 5: Steps in solder joint formation

2.4.2 Fundamental of Soldering

Soldering is defined as joining of two or more solderable metal surfaces, i.e. Metal Surface 1 (e.g. PCB Surface) and Metal Surface 2 (e.g. plated coating on a component lead), by introducing a third low molten alloy that reacts in molten state with the solid metal surfaces to be joined.

In a soldering process, the solder melts and fills the space between the two metal surfaces and bonds to them by wetting action. When the soldering process is completed, Inter-Metallic Compounds (IMC's) are formed at the interfaces of solder and the metals as illustrated in figure 6.

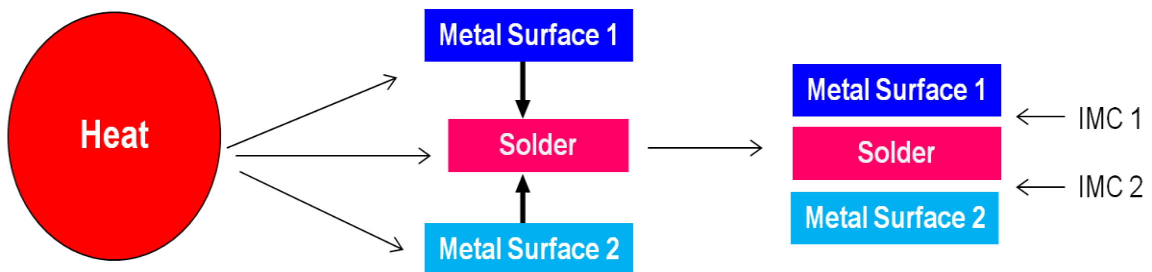

Figure 6: Interrmetallic formation (Doss, 2011)

المنارة للاستشارات
www.manaraa.com

2.4.3 Soldering Mechanism

Soldering process is summarized in 9 steps in table 2 below.

Table 2: Soldering mechanism (Doss, 2011)

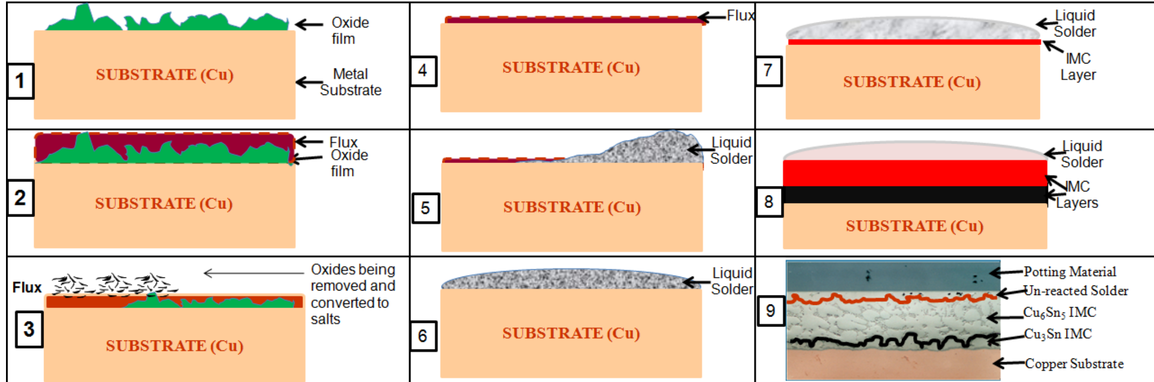

In step 1, the figure depicts initial state of the metal surface with non-uniform oxide film. In step 2, a flux is applied to the metal surface. In this figure, the metal surface with a thin non-uniform oxide film and a thin layer of flux is seen. In step 3, the oxide film is being removed by the fluxing action as this surface is heated. The figure on the left shows the presence of some left-over oxide and the porous organic- metallic salts on the surface. In step 4, the oxide film is now completely removed by the flux. The figure shows a metal surface and a thin continuous layer of flux. In step 5, liquid solder is in direct contact with the metal surface. One can see a very thin film of flux on the exposed bare metal surface along with liquid solder. In step 6, liquid solder spreads across the entire metal surface forming a thin convex coating with low wetting angle thereby showing a good wetting. In step 7, the metal surface is completely wetted by the liquid solder. Intermetallic Compound is beginning to form. In step 8, adhesion of the solid solder alloy to the base metal is complete with the formation of two intermetallic compounds, Cu_6Sn_5 and Cu_3Sn. Finally, step 9 clearly show a real world example of

المنارة للاستشارات
www.manaraa.com

different parts of a solder joint. The solder joint here shows the copper substrate with Cu_3Sn IMC, followed by Cu_6Sn_5 IMC and some un-reacted solders.

المنارة للاستشارات
www.manaraa.com

CHAPTER 3: ELECTROCHEMICAL MIGRATION

3.1 ECM Definition

ECM is defined as the "growth of conductive metal filaments or dendrites on or through a printed board under the influence of a DC voltage bias" (IPC, 1997). However this definition is too narrow to cover the characteristic and physical movement of metal involved. Thus, many researcher in industry redefine ECM as:" the movement of metal ion through an electrolytic solution under an applied electric field between dielectric insulated conductors" (Hilman, 2010). ECM can occur on or in almost all electric packaging including die surface, epoxy encapsulant, and passive components. ECM is known to be accelerated by excessive ionic contamination owing to insufficient cleanliness.

3.2 ECM Mechanisms

Dendritic growth and conductive anodic filaments (CAF) are two common ECM mechanisms. Dendrite growth is a descriptor for ECM along a surface that produces a dendrite morphology such as "tree-like" or "Feather-like" form. CAF is beyond the scope of this study and thus will not be described. The traditional electrochemical migration of metal involves the following steps:

Step 1: Creation of an electrolytic solution containing sufficiently conductive metal ions in a humid environment in presence of ionic contaminants.

Step 2: Electro-dissolution of metal in presence of positive electric field and an electrolyte.

المنارة للاستشارات
www.manaraa.com

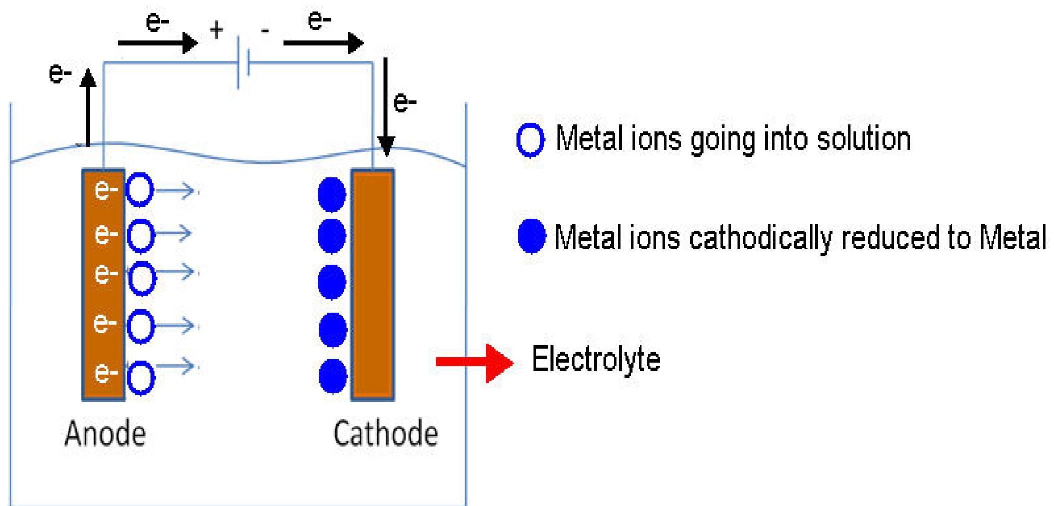

Figure 7: Electrochemistry of ECM

This step usually occurs adjacent to anode, e.g.

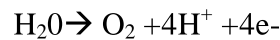

$$H_20 \rightarrow O_2 + 4H^+ + 4e-$$

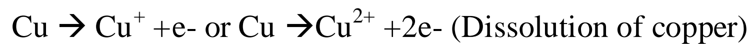

$$Cu \rightarrow Cu^+ + e- \text{ or } Cu \rightarrow Cu^{2+} + 2e- \text{ (Dissolution of copper)}$$

Step 3: Migration of charged particles through a solution under the influence of an electric field

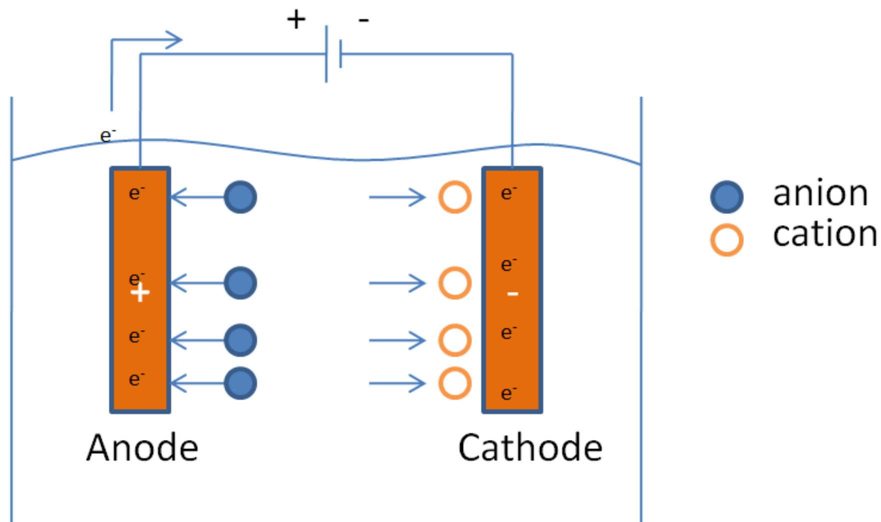

Figure 8: Ionic migration

المنارة للاستشارات
www.manaraa.com

In figure 8 the positive ions travel along the field lines (in solution) from anode to cathode while electrons travel from cathode to anode, a reverse direction in the external conductor.

Velocity can be computed as follows:

$$v = \mu * E \ where \ \mu = \frac{q}{(6\pi r\eta)}$$

v: velocity (m/s)

E: field strength (V/m)

μ: mobility (m^2/[Vxs])

q: electron charge (C)

r: ionic radius (m)

η: viscosity (m^2/s)

Step 4: Electro-deposition occurs once ions reach the cathode. The cathodic reactions are represented as follows:

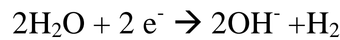

$2H_2O + 2e^- \rightarrow 2OH^- + H_2$

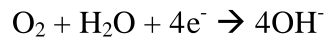

$O_2 + H_2O + 4e^- \rightarrow 4OH^-$

$Cu^+ + e^- \rightarrow Cu$ or $Cu^{2+} + 2e^- \rightarrow Cu$

The rate of deposition of metal ion depends on the metal ion concentration in the aqueous solution because cathodic electrodeposition is largely diffusion controlled. However, the production of hydroxyl ions (OH-) at cathode can reduce the rate of Cu deposition by combining metals ions with hydroxyl ions to form insoluble hydroxides. Thus ECM rate is correlated with solubility product of the metal ion with hydroxide (Hillman, 2010). Furthermore, ionic contaminants (such as Cl^-) can change the ECM rate

المنارة للاستشارات
www.manaraa.com

by forming alternate reaction paths and forming additional ionic species. For example, $CuCl_2$ can form two electrons, Cu^+ ,and Cl^-.

3.3 ECM Drivers

There are two main drivers that lead to ECM: voltage/electric field and contamination. Time to failure modes will provide a more quantitative understanding of these primary drivers.

3.3.1 Voltage and Electric Field

Voltage is primary drivers for the two processes, namely, electro-dissolution and ion migration. IPC-2221A allows 15V/mil on copper traces. Based on the study of DfR, using IPC-B-25 coupons with NaCl, dendritic growth occurs at 6V/6.25 mil (0.96V/mil) space and does not occur at 42V/25 mil (1.68V/mil) which defines the combination of electric filed and spacing to initiate ECM (Hilman, 2010). Some studies have shown that the occurrence of ECM is strongly driven by the electric field strength (L. Zou and C. Hint, 1999), (E. Bimiller and C. Hillman, 2004).

3.3.2 Contamination

Ionic contaminants are of two different types: insoluble in water such as AgCl and soluble in water like NaCl. The greatest concern is that ionic contaminants are very common in electronics manufacturing process because of the formation of anions and cations during the interaction between components and PCB metallization with manufacturing process chemicals.

Some of the sources of contaminants in printed board fabrication processes are: rinse water, fluxes, handling, and storage and use environment. There are many processes during PCB fabrication which can result in accumulation of contaminants on the board.

المنارة للاستشارات
www.manaraa.com

Etching, neutralizer, cleaning, photoresist stripping and electroless plating are examples of the processes during PCB fabrication that can leave behind ionic contaminants.

3.3.3 Time to Failure Models

Failure models can provide a more understanding of the primary drivers quantitatively of ECM. Many models have been used in the electronics industry but no one has established the benchmark of time to failure for specific circuit boards because of the unpredictable drivers of ECM. Below are the potential time to failure models that based on chemical kinetics.

3.3.3.1 Arrhenius Model

The Arrhenius model is based on the fundamental chemical behavior

$$t_f = A \exp\left(\frac{\Delta H}{kT}\right)$$

A : scaling constant,

ΔH : activation energy (eV),

k : Boltzmann constant (8.62 x 10^{-5} eV/K)

T : temperature (K)

The model was widely used to describe variety of chemical reaction but is limited to temperature effects. Because of that Hornung (Hornung, 1968) proposed a mathematical model which is

$$t_f = \frac{\alpha G}{V} \exp\left(\frac{\Delta H}{kT}\right)$$

α : proportionality constant

G : electrode spacing

V : voltage

المنارة للاستشارات
www.manaraa.com

ΔH : activation energy (eV)

k : Boltzmann constant (8.62 x 10^{-5} eV/K)

T : the applied temperature (K)

Based on the dendritic growth of silver through borosilicate glass under an electric field , he found activation energy is 1.15 eV which linearly correlated with dendritic growth rate. The Arrhenius and Hornung equations are derived from assumptions based around elastic collisions and kinetics reaction rate. (Hilman, 2010)

3.3.3.2 Barton and Bockris (J. Barton and J. Bockris, 1962)

In 1962, Barton and Bockris published the model of growth of dendrite in electrolytic solution

$$t_f = \frac{h8\gamma RT}{F^2 D c_\infty \eta^2}$$

h : conductor spacing

γ: interfacial energy

R : universal gas constant

T : temperature

F :Faraday constant

D: diffusion coefficient

c_∞: metal ion concentration,

η :overpotential

i:current density at the dendrite tip

The Barton and Bockris model is a good general model for dendritic growth but it only applies when the dendritic growth is the rate limiting step and includes no terms for

المنارة للاستشارات
www.manaraa.com

path formation, electrodissolution, and ion transport. Nevertheless, the model is based on the experimental observations of dendritic growths, thus has some predictive ability.

www.manaraa.com

CHAPTER 4: EXPERIMENTAL METHODS

4.1 Characterization Technique

4.1.1 Cross-Sectioning

Cross-sectioning is one of the failure analysis techniques that allows for in-depth analysis of the inner layer of chips or any subjects from PCB by mechanically exposing a plane of interest in a die or package. Cross-sectioning procedure consists of sample preparation, grinding, polishing the specimen until the plane of interest is ready for optical or electron microscopy. Conventional micro-sectioning starts with sample preparation. This consists of sawing and mounting which involves the encapsulation of the specimen with an epoxy or acrylic material. When excising the specimen out of the circuit board, it is always a good practice to saw or cut as close as possible to the target to ensure it will fit inside the mounting cup, as well as to reduce the grinding needed during actual sectioning. Thus, once the sample is cut and cleaned, it's critical to position the specimen in the mold correctly. The mold is to help to hold the specimen intact and provides a better handle on the component during grinding and polishing.

Figure 9: Example of a sample mounting mold

المنارة للاستشارات
www.manaraa.com

A mix of hardener and resin is usually poured inside the cup slowly to avoid bubbles as much as possible. Based on the total volume of material needed and the mixing ratio specified, one calculates how much of hardener and resin is needed. One stops mixing when the epoxy is transparent and homogenous. The sample is then carefully moved into a desiccators equipped with a vacuum pump to allow the epoxy to fill all gaps and the air bubbles to rise to the top. The final step of preparation is to allow the epoxy cure at ambient pressure.

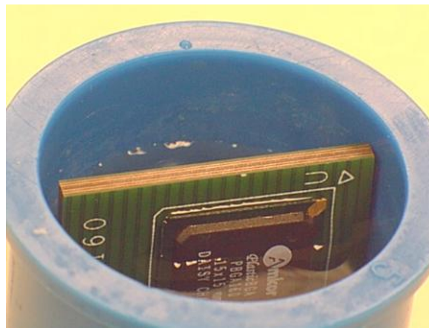

Figure 10: Illustration of epoxy being poured into the mounting cup/mold

The next sample preparation step is grinding of the encapsulated specimen to the point of interest. A typical grinder/polisher has a platen (or a set of platens) over which the grinding material (Sic paper, polishing cloth, diamond paste, etc.) is placed. The five grit sizes used are 320, 400, 600, 800, and 1200. If the cross- sectioning component contains ceramic or similar material, one grinds the specimen on 70 micron and 60 micron metal bonded diamond-grinding disc until reaching the target plane. The specimen then is washed and cleaned in a methanol ultrasonic bath. If the cross-sectioning component contains non-ceramic components, one starts grinding with 320 grit paper , then 400 grit paper when 3-4 mm of thickness is left between the grinding plan and the target feature.

www.manaraa.com

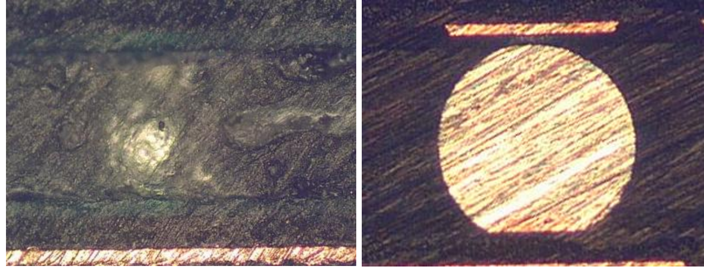

Figure 11**:** The images (from left to right) of the target areas at 320 and 400 grit papers. (Jabil)

One washes the sample with water and continues grinding with 600, 800, and 1200 grit paper to reach the center of the designed feature.

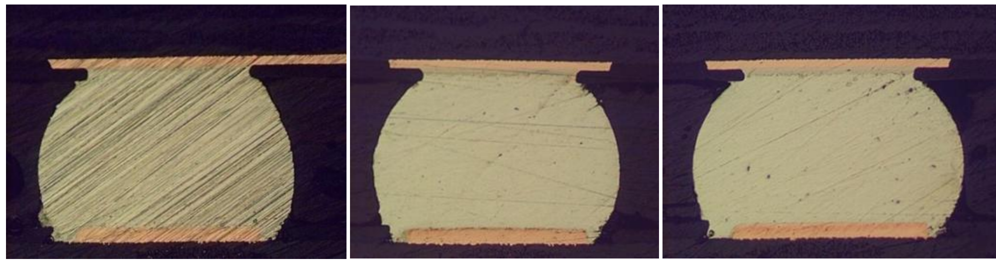

Figure 12**:** The images (from left to right) of the target areas at 600, 800, and 1200 grit papers. (Jabil)

Polishing follows grinding. Polishing is very similar to grinding which involves the use of fine abrasive suspensions and several different polishing pads to produce a mirror finish. Rough polishing is usually done using 3 micron diamond particles. Fine polishing is usually done using 1-micron, then 0.05-micron alumina particles (Siliconfareast) (B. Engel, E. Levine, J. Petrus, and A. Shore, 2004).

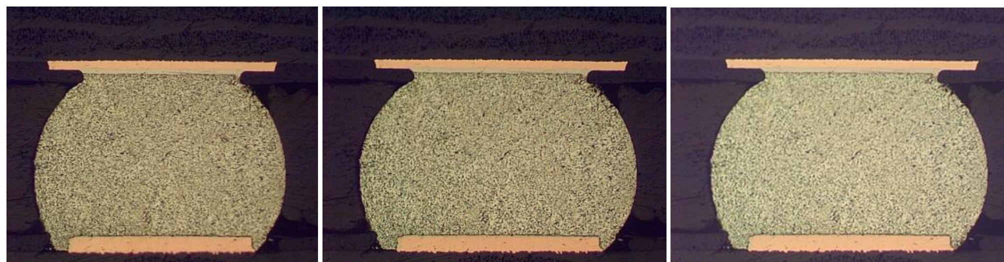

Figure 13**:** The images (from left to right) of the target areas after polishing with 3.0, 1.0 and 0.05 micron colloidal silica suspensions (Jabil)

المنارة للاستشارات
www.manaraa.com

4.1.2 Ion Chromatography

Ion chromatography is an analytical technique used for analyzing anions such as fluoride, chloride, nitrite, nitrate, sulfate, phosphate as well as organic acids in part per million (ppm) quantities in aqueous solutions. It is one of the members of large family of analytical tools that comes in many forms, e.g., paper chromatography, liquid chromatography, gas chromatography, high pressure liquid chromatography, but all of these employ the same basic principles.

The ion chromatography method is defined by a separation mechanism and a detection method. The separation mechanism is a column that consist of ion exchange resins. The usual chemical group for cation-exchange resin is either sulfuric or carboxylic acids while ammonium group is for anion separation exchange. The separation happens between two phases: stationary phase and a mobile phase. Figure 14 show the process of ion exchange :analyze ions are marked A and eluent ions are marked E. Eluent ions from the eluent solution are used to extract the analyze ions out of its solution. Both A and E compete with each other for the exchange positions.

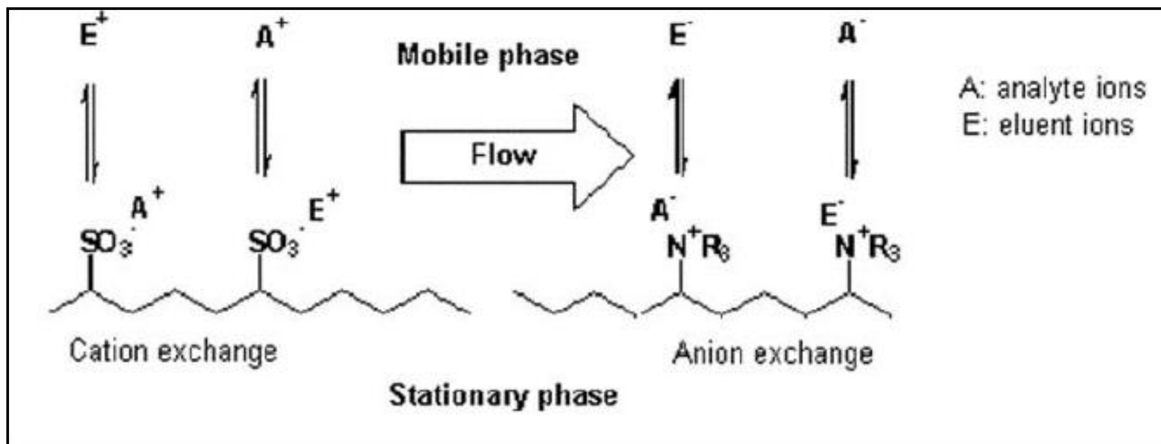

Figure 14: Schematic diagram showing the ion exchange process (Eith, 2001)

المنارة للاستشارات
www.manaraa.com

Below is the cation exchange with sulfuric acid group reaction:

$$-SO_3^- H^+(s) + Mx^+(aq) \rightleftharpoons -SO_3^- Mx^+(s) + H^+(aq)$$

M^{x+} : the cation of charge x.

(s) : the solid or stationary phase.

(aq) : the aqueous or mobile phase.

The equilibrium constant is

$$Keq = \frac{[-SO_3^- Mx^+]s\,[H^+]aq}{[-SO_3^- H^+]s\,[Mx^+]aq}$$

The length of time that resin is retained in the column depends on the value of Keq. Adjusting the pH ([H+]aq) helps control the time cation extracts from column .

Ions are separated and flown through mobile phase will be then detected by measuring the conductivity of the solution using a conductivity cell. Because mobile phase contains ions that create a background of conductivity, an eluent suppressor which consist of a ion exchange column or membrane, is used to convert the mobile phase ions to a neutral form. For cation analysis, the eluent suppressor supplies OH- to neutralized common group such as HCl, or HNO_3. For anion analysis, the eluent suppressor supplies H+ to neutralize the anion.

Figure 15 is the sample output data of ion chromatography. Each peak represents an ion from sample solution and the height of each peak correlates to the concentration of each ion moving through the column at a particular time which is called elution time.

www.manaraa.com

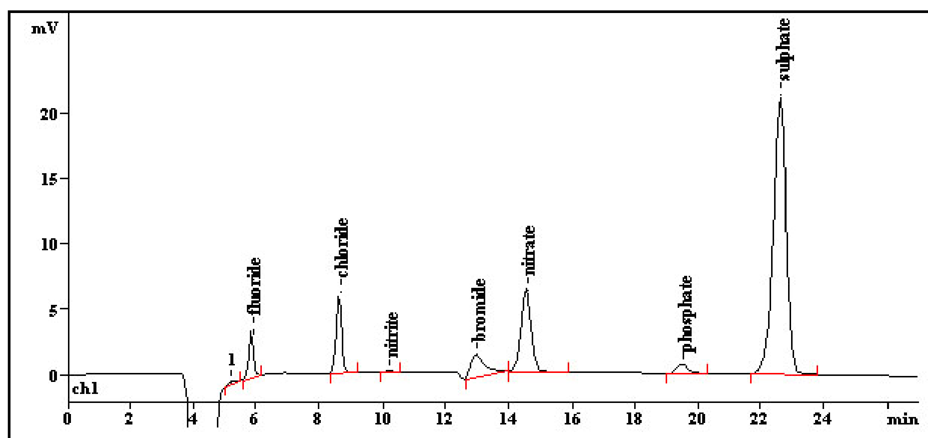

Figure 15: Ion chromatography data from an anion analysis of glacial water (Bruckner)

Ion chromatography has been used extensively and has become a powerful tool in the semiconductor industry, especially in the identification of contaminants that cause yield and quality issues. This is because it can provide quantitative analysis of anions in the ppb range, making it capable of detecting contaminants on the surface of a wafer, die, or package. Since ionic contamination is a major source of corrosion problems in the industry, ion chromatography is considered to be an indispensable tool when analyzing water samples suspected to be the cause of corrosion issues on the PCB.

Figure16: Ion chromatography

المنارة للاستشارات

www.manaraa.com

4.1.2.1 Ion Chromatography Preparation

Tested solution is prepared by one of two technique options: (a) localized extraction - to extract residues at specific locations; (b) bag extraction – to extract residues from the entire PCB assembly.

4.1.2.1.1 Localized Extraction

Localized extraction (LE) is a process of extracting residues at specific locations on the PCB assembly. It can function as a localized cleanliness tester. By performing the electrical test that is a predictor of field performance based on ionic cleanliness, LE gives ‘Clean’ or ‘Dirty’ reading. The extracted sample can be used for follow-up analysis to determine what contaminants and their amounts are present. LE method helps in extracting ionic contaminants from PCB surfaces. Figure 17 shows the picture of a localized extraction set up used in the current thesis work.

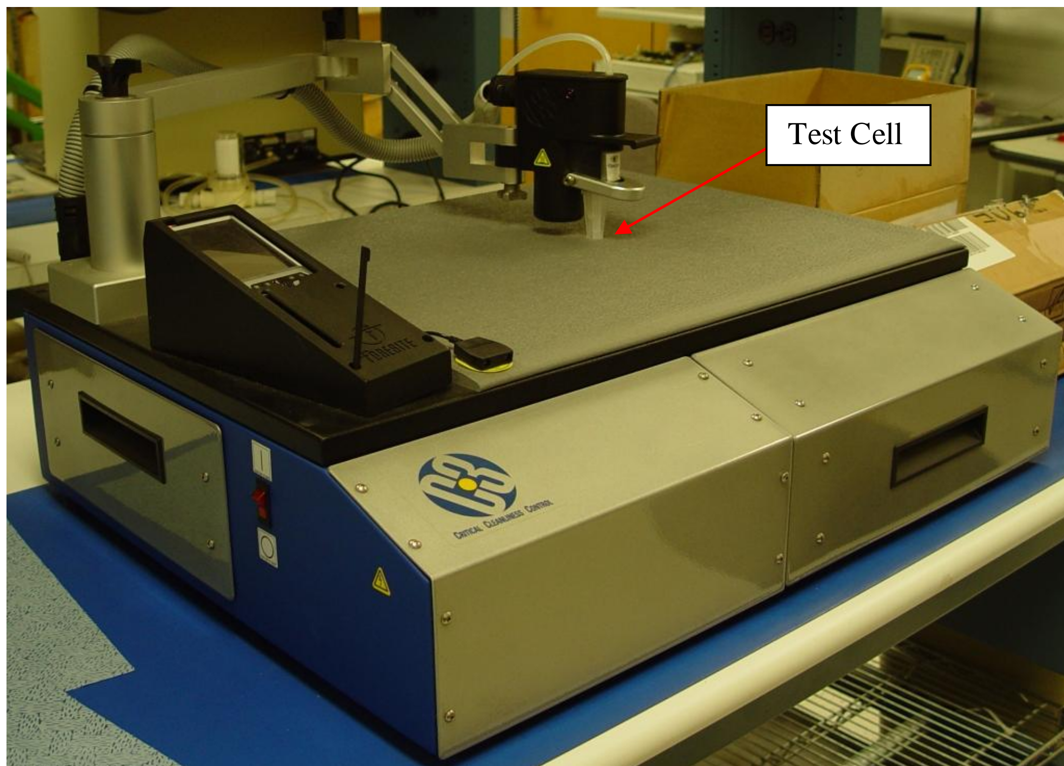

Figure 17: C3 cleanliness tester-localized extraction

المنارة للاستشارات
www.manaraa.com

The test cell area (see in figure 18) is 10mm dia. circle / 0.7 sq. cm.; the footprint required is 16mm dia. circle / 2.0 sq. cm. The test cell is specifically designed to collect 24 ml of solution. The extraction process has been designed to achieve effective ionic residue removal using the following 3 steps per cycle:

1: Solution heating / delivery to the extraction site (see the red arrow in figure 18).

2: Soak and solubilization time at the bottom area of the cell (see the yellow in figure 18).

3: Aspiration of solution to collection cell (see the blue arrow in figure 18).

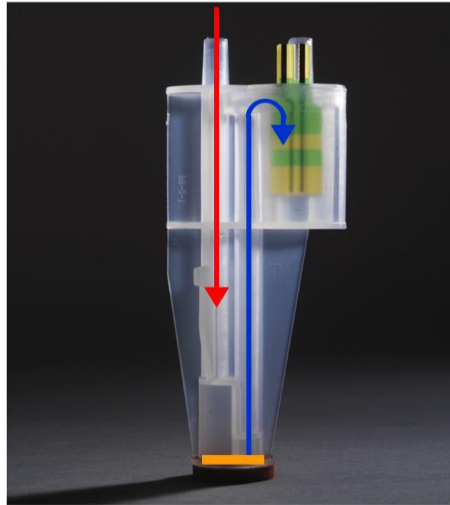

Figure 18: C3 cleanliness test cell (Foresite)

This cycle is repeated 9 times to ensure effective residue removal. Generally, the testing is basically based on the assumption that a more corrosive ionic species will cause electrical leakage event to occur more quickly; insulative residues take longer to cause a leakage event.

المنارة للاستشارات
www.manaraa.com

4.1.2.1.2 Bag Extraction

Bag extraction is a process for extracting the residues from the entire PCB assembly. This process is employed to test the overall cleanliness of a board. There are three important steps to this process. First, the board needs to be enclosed by a clean plastic bag as shown in figure 19. Second, a mixture containing 75% Isopropyl Alcohol (IPA) and 25% Dionized Water (DI) is placed in the plastic bag to cover the entire PCB area. Third, one hour heating at 80°C is applied to the whole package using precision heating equipment.

Figure 19: Bag extraction process

The 75/25 of IPA/DI water solution is recognized as an acceptable fluid by IPC to extract the residues from the PCB assembly. The theory is that the alcohol/water mixture dissolves all the flux residues from the boards and the reaction rate is increased by heating up to a higher temperature. The extraction solution is used for ion chromatography after one hour of cooling.

4.2 Test Vehicle Design

The test vehicle was a specially designed PCB to perform water drop test. between two conductor pads in condensed moisture environment at room temperature. It was designed per IPC-A-600 specification.

المنارة للاستشارات
www.manaraa.com

The design process was divided into two steps. The first step was to design the test cell. Second step was to design the board's layout. The table 3 below shows the designed parameters and variables for this experiment.

Table 3: Test vehicle PCB design parameters and variables

Variables	**Parameters**
Number of spacing	Cell Diameter
Surface Finish	Cell Thickness
Pad Size	Volume of test solution

Figure 20 shows the details of the test cell design. The test cell structure is standardized per IPC-A-600 and has five layers. Layers structure were copper layer one, dielectric layer one (FR4),solder mask layer, the copper layer 2 (FR4), and dielectric layer 2. Also, the top of copper pad was processed through hot air solder leveling technique (HASL) to coat the PCB pads with solder alloy. The cross-sectioning characterization process showed the HASL covered the entire copper pads. This was done to eliminate interference in the electrode reactions from the base metal copper.

In figure 20, 'x' is defined as the spacing between two copper pads, while 'a' is the width of copper pad. The width of the pad is maintained constant at 50 mils. The diameter of test cell is 8 mm. The depth of the cell starts from copper layers 1 to copper layers 2 is 1.5 mm.

المنارة للاستشارات
www.manaraa.com

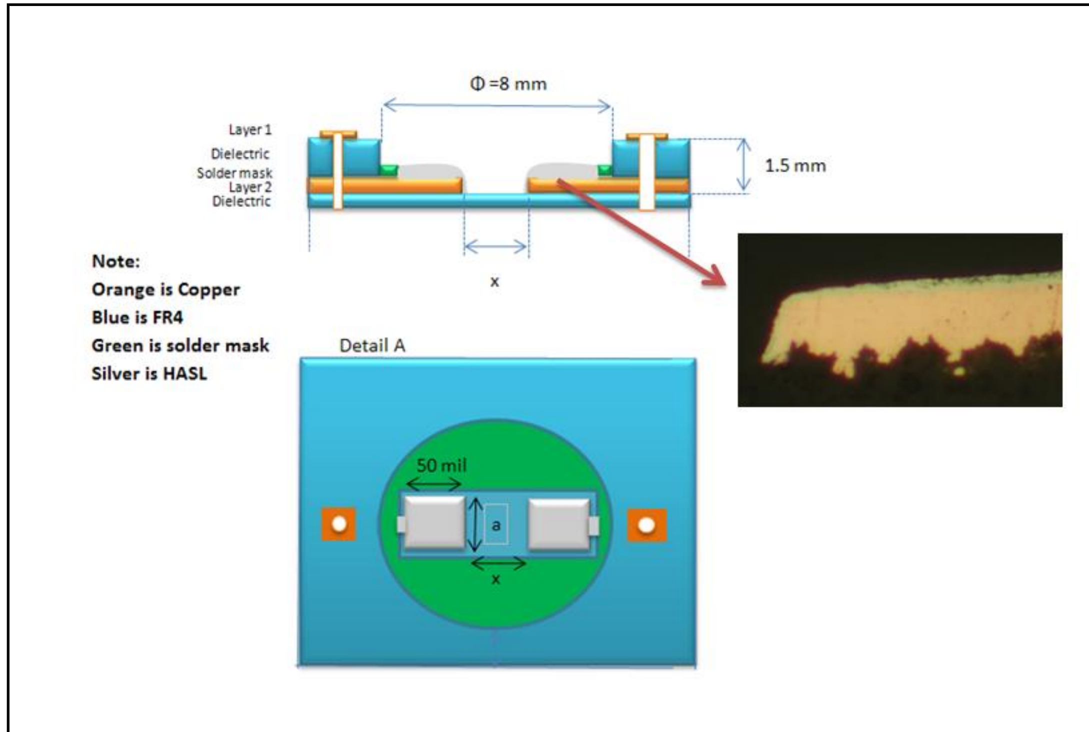

Figure 20: The cross-sectioning of test cell structure

Table 4 shows the various design spacing between pads ('x') and Pad length ('a') on the test cell. There are five different pad spacings and widths in order to have a variety of options as much as possible. But in this investigation, the purpose to this research may only focus on the specific spacing and width.

Table 4: Test PCB pad design

PCB Pad Spacing, (x), mils	**Pad Width (a), mils**
6.25	50
12.5	70
25	90
37.5	110
50	130

المنارة للاستشارات
www.manaraa.com

The table 5 below summarizes the test cell materials used in the ECM experiments.

Table 5: Test cell materials

Surface Finish	**Board Material**	**Pad Material**
Tin-Lead HASL	FR4	Copper
Lead Free HASL	Solder Mask	

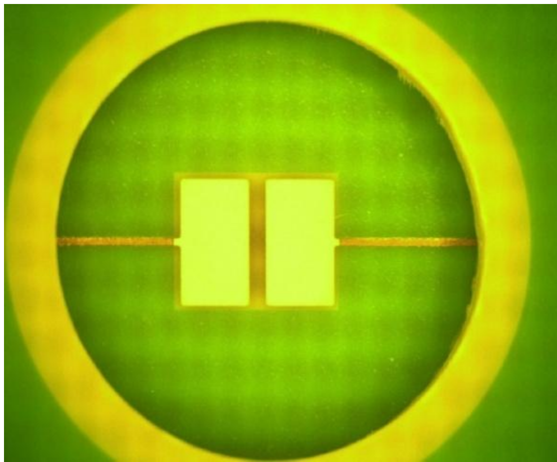

Figure 21: Fabricated lead free cell

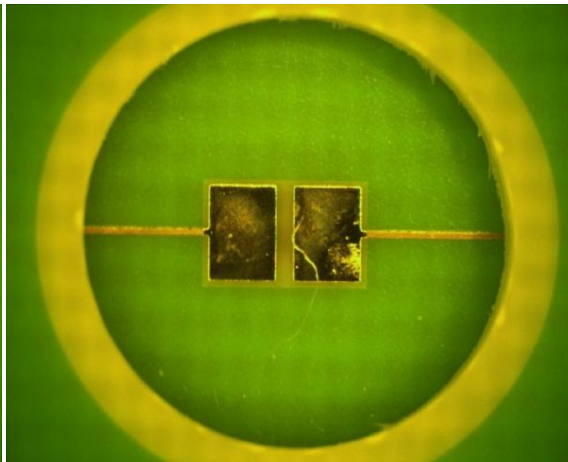

Figure 22: Fabricated tin-lead cell

Figure 21 and 22 are examples of lead free and tin-lead cells. Each of these boards consist of 20 test cells as shown in figure 23. The row of the board corresponded to the different dimension of the copper pad while the columm corresponded to the different spacings between copper pads as shown in the table 5 above.The board dimensions are 5.8”x2.2” and contains 20 cells with identical 8 mm diameter, 1.5 mm deep cavities.

المنارة للاستشارات
www.manaraa.com

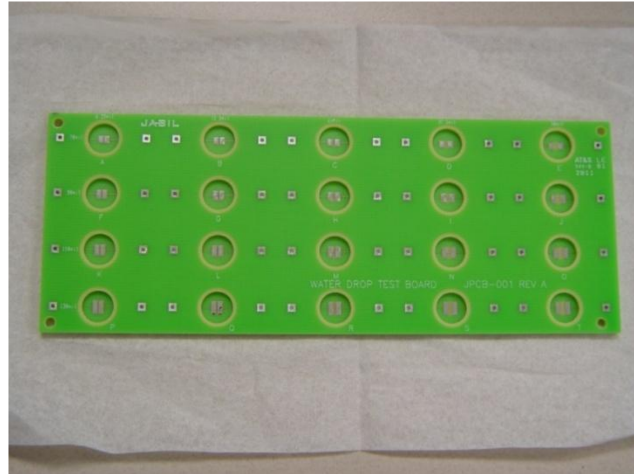

Figure 23: Completed fabricated test vehicle layout

4.3 Water Drop Test Procedure and Setup

Before doing the water drop test it is important to set up the right circuitry which is crucial in collecting the right data. Therefore, the equipment and material used had to be tested and calibrated before using. The following equipment and materials below were needed for running the test.

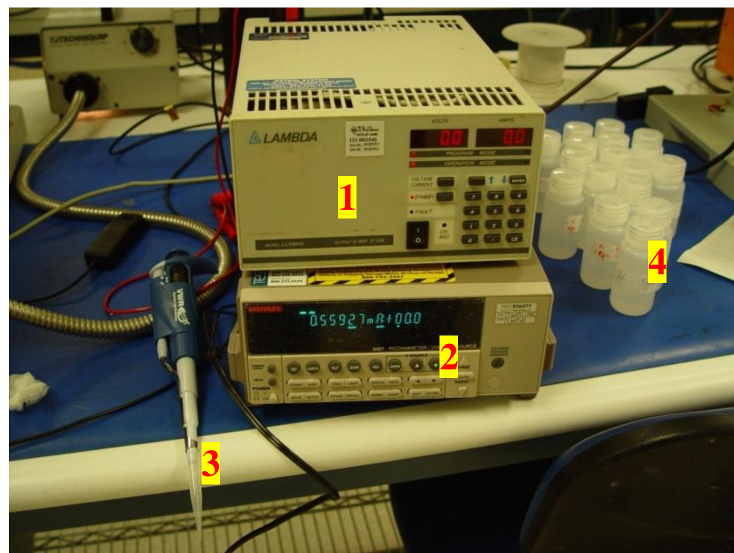

Figure 24: Water drop test equipment set up: (1) power supplier-lambda LLS8040, (2) keithley picoammeter, (3) pipetter, (4) anion samples

المنارة للاستشارات
www.manaraa.com

Figure 25: Water drop test equipments set up: (5) CRT monitor, (6) computer screen (with excel data display)

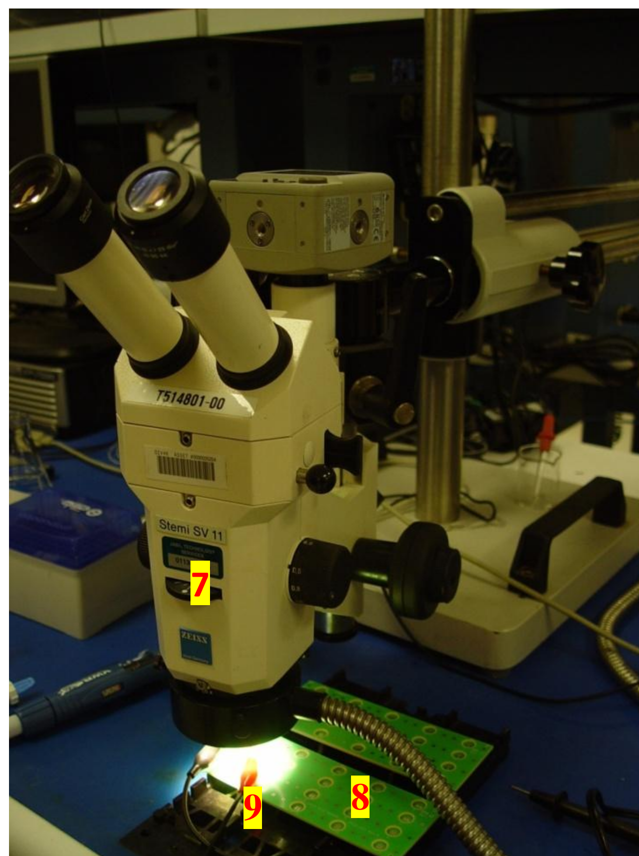

Figure 26: Water drop test equipments set up: (7) microscope, (8) test vehicle board, (9) gator connector cable

المنارة للاستشارات
www.manaraa.com

The procedure to perform WDT is shown below. First, one places the board for viewing under the microscope, so that the parallel conductors are in view. One then uses the eye dropper, places a drop of liquid sample across the conductors that are in view under the microscope, and at least 0.5” away from the place where external wires are attached to parallel conductors. Secondly, one connects USB interface into computer and turns Keithley unit on, then opens excel and clicks on add-in ExceLINX to create “Configure Meter” worksheet and select device “KE6485_COM2”. One makes sure to "Change Status/Cmd" to “Detect Device” on worksheet and clicks on ExceLINX add-in. The "Status/Cmd" should change to “Running” then say “Task Stopped Successfully” with an updated device reading KE6485_COM2*. Finally, one changes data in worksheet to reflect the test parameters need to run test. Figure 27 is the connection chart of the equipment and material: A voltage is applied to the test cell. A picoammeter is connected in series with voltage supplier. A computer software is connected with picoammeter to record the current.

To avoid fault data, these are a few things need to consider during testing. First, one makes sure all electrical cables are connected probably. Second, one needs to keep an eye on the microscope to visually see the ECM form and keep tracking the record. Finally, one is required to wear nitrile glove to prevent contamination and anti-static protection.

www.manaraa.com

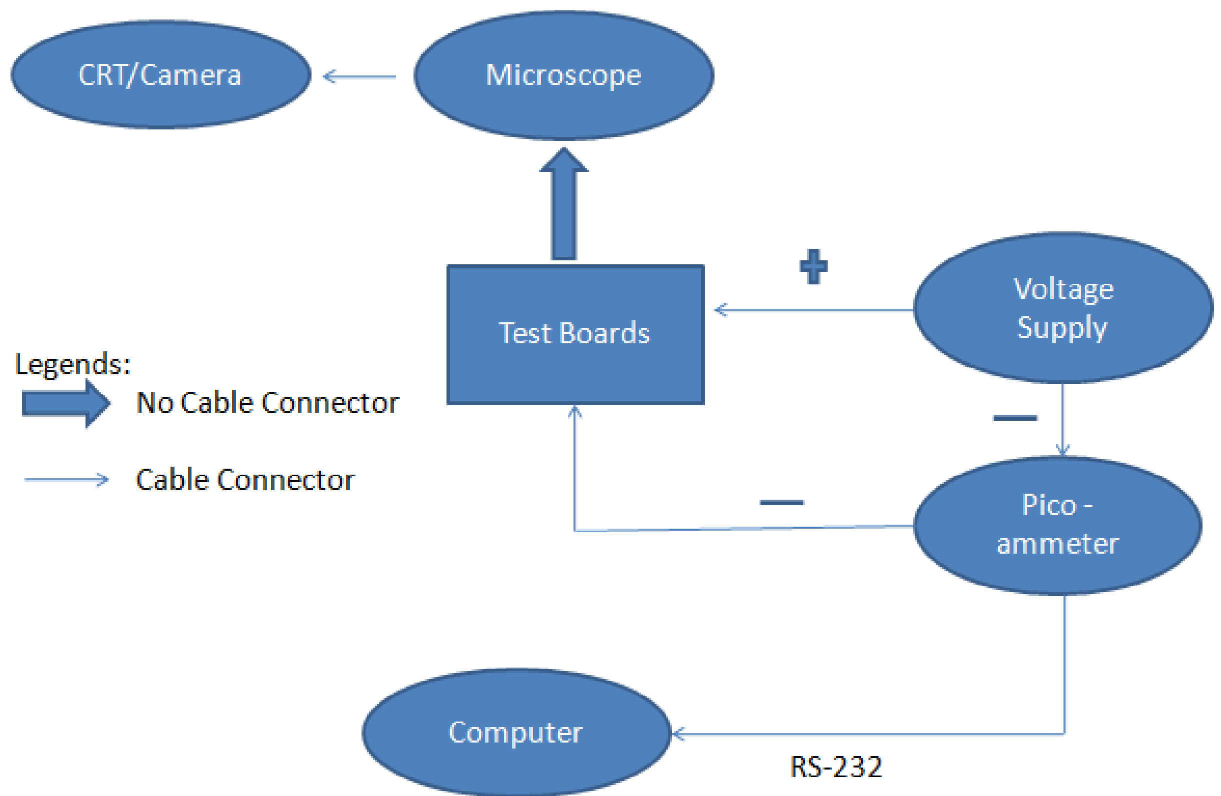

Figure 27: Flow chart illustrating set up procedure

4.4 Design of Experiment

The design of experiment (DOE) has three factors which are anion type, pad spacing, and surface finish. Only three common inorganic acid anions are tested: chloride, bromide, sulfate, and one organic acid anion: succinate. The spacing factor has tested with two levels of 12.5 mil and 25 mil which represent the most common design spacings in PCB in the industry. The surface finishes are tin-lead HASL and lead free HASL. The experiments are replicated five times. The total DOE run is 90 in 45 boards. The output of this DOE is to investigate on how the current of the individual anions and their interaction that affect the time to failure on PCB. Thus the outcome of this DOE is measuring current and time to failure . Table 6 summarizes the DOE matrix.

المنارة للاستشارات
www.manaraa.com

Table 6: DOE parameter matrix

Factors	Levels				Replicate	Responses
	1	2	3	4		
Anions	Cl^-	Br^-	SO^{4-}	Succinate	5	Current and Time to Failure
Spacing	12.5	25				
Surface Finish	Tin Lead	Lead Free				

*Detailed run matrix is shown in Table 8, section 5.2.2

4.5 Cleaning Process

In order to evaluate the "as received" boards, a simple DI water drop test was performed. If dendritic growth occurs in less than 180 seconds, the "as-received" boards are not clean enough to be used as starting material for the experimental study.

In order to judge the level of "as received" contamination, WDT is done on "as-received" boards with DI water. If the board does not have circuit short fast less than 180 s (as an estimation), one can proceed with DOE matrix as planned in table 6. If the board has circuit short fast less than 180 s, bag extractions is proceeded using IPC-TM-650, method 2.3.28 with 75% IPA, 25% DI water mixture or 100% DI water, both at 80°C for one hour. Once one decides which bag extraction solution extracts the contamination more effectively, all boards are cleaned with the same process which requires for a repeatable experimental data. Figure 28 shows the cleaning process.

المنارة للاستشارات
www.manaraa.com

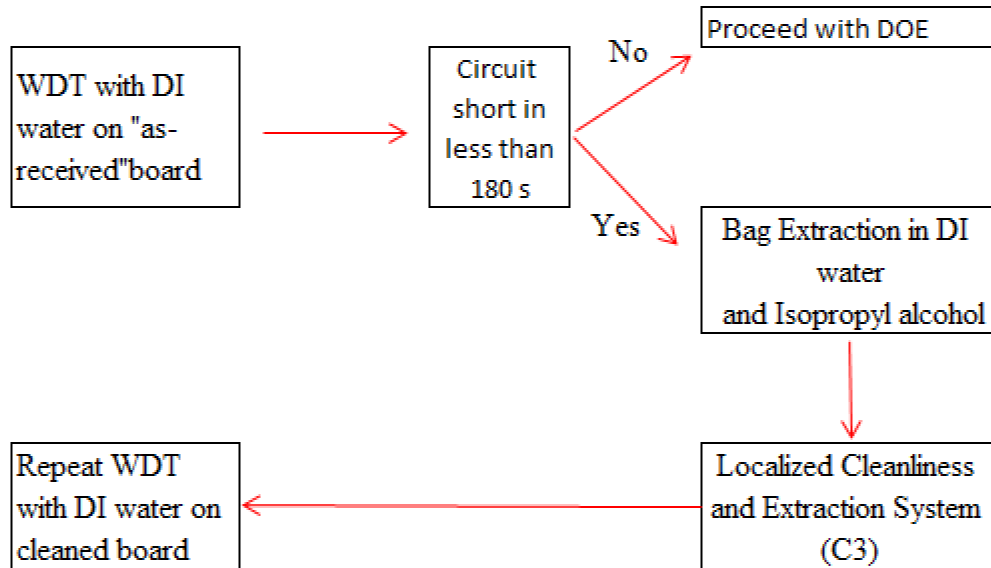

Figure 28: Cleaning process flow chart

4.6 Water Drop Test

The WDT procedure was performed per IPC TM650, 2.6.1. In this study, a pipetter was used to dispense 140 µl of each test anion at an optimized concentration into the 12.5 mil or 25 mil spacing test coupon cell having different surface finishes: Sn-Pb and Pb free HASL. The field strength applied was a constant 0.5v/ mil. Current and time was monitored during the test.

Anion concentrations were optimized to achieve dendritic short failures within a time window of 0 to 180 seconds. This was accomplished by trying different concentrations of each anion and selecting the concentration which produced dendritic shorts within the prescribed time window.

المنارة للاستشارات
www.manaraa.com

Because of the differences in anion activity, the concentrations used varied from one anion to another. Table 7 below summarizes the concentrations of each anion.

Table 7: DOE matrix for concentration

Anions	Cl^-	Br^-	Sulfate	Succinate*
Concentration (ppm)	3	15	2	1000

* Succinate is not used in the final DOE owing to an absence of ECM in the entire range of concentrations tested (see figure 32 for further details).

Figure 29 shows the electrochemical migration on tin-lead board after applied 0.5 v/mil of field strength and 140 µl of Br- solution. The tree-like structure creates the bridge between two pads that lead to a short circuit. The bubble on the figure maybe the result of competing cathodic electrode reaction involving hydrogen gas evolution. The white pattern indicates the formation of white crystalline deposits on the cathode which inhibited cathodic reduction of tin ions.

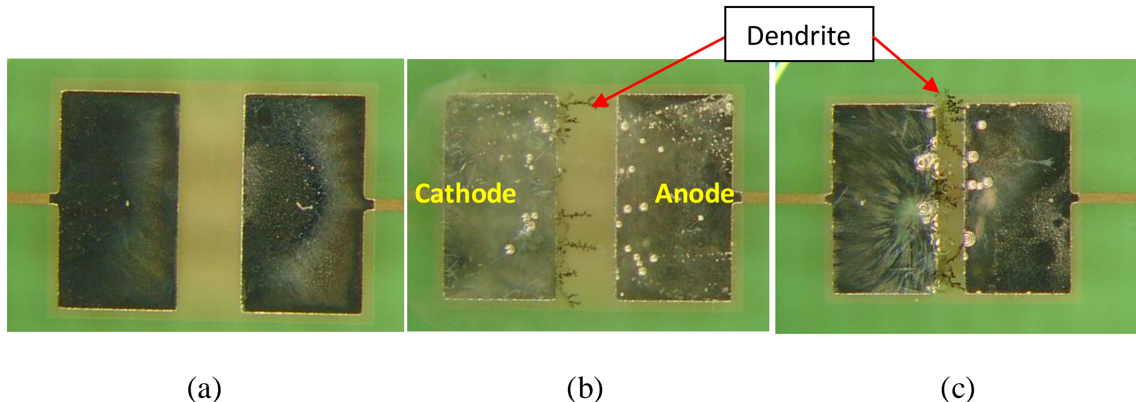

(a) (b) (c)

Figure 29: Electrochemical migration of Br- on tin-lead board: (a) virgin board, (b) ECM growth, (c) ECM bridge

المنارة للاستشارات
www.manaraa.com

Figure 30 shows the electrochemical migration in the presence of Br-, while applying the same field strength and volume of solution as above on a lead- free board. Within 180 second under constant voltage, the tree-like structure appears and creates a bridge between the two pads. Once the dendrite reaches the other side of the electrode, a short circuit develops.

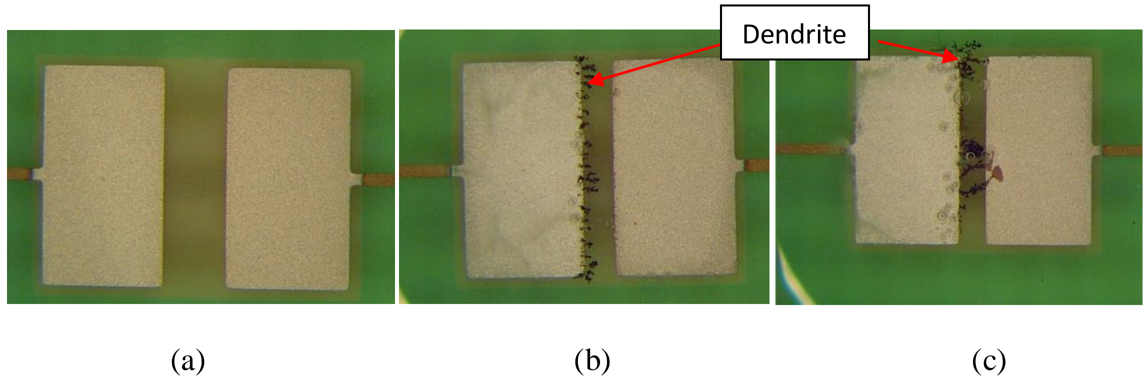

(a) (b) (c)

Figure 30: Electrochemical migration of Br- on lead free board: (a) virgin board, (b) ECM growth, (c) ECM bridge

The same experiment is repeated as described in table 7 for different anions. The same result is repeated as figure 29 and 30 but occurs at a different rate. In chapter 5, these results are discussed in detail with respect to time to failure for each test coupon.

المنارة للاستشارات
www.manaraa.com

CHAPTER 5: RESULTS

5.1 Cleaning Process Result

To evaluate the as received boards, a simple DI water drop test was performed. Surprisingly, dendritic growth occurred quickly in less than 180 seconds. This showed that the as-receive boards were not clean enough to be used as starting material for the experimental study. A C3 extraction of four cells on each cleaned tin-lead and lead free board was done. Then the C3 extract solution was analyzed by ion chromatography for total anions. Ion Chromatography results were presented in figure 31. The overall total anions detected were lower in the DI water cleaned boards than the 75/25 IPA/DI cleaned boards. Repeating the DI water WDT test on DI water cleaned boards did not produce a failure. On the basis of these results, all the boards were cleaned with DI water using IPC's extraction parameters.

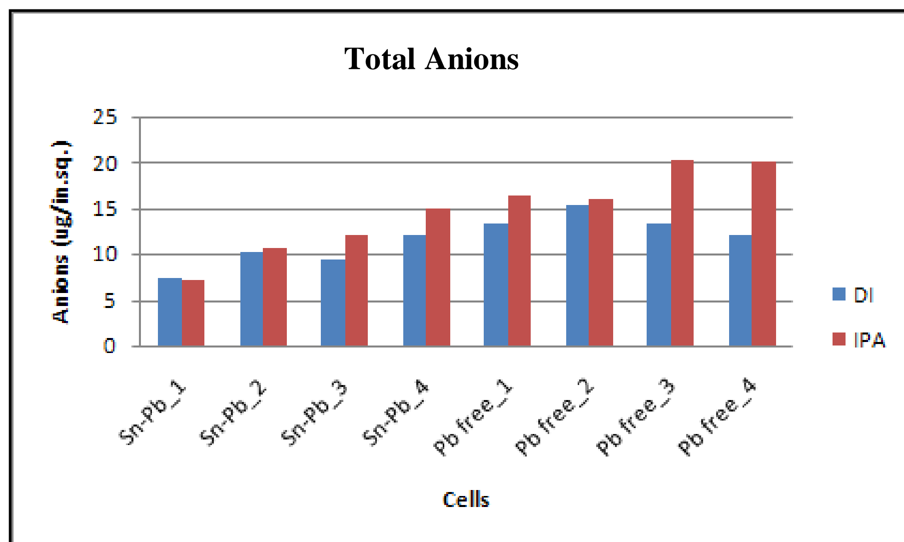

Figure 31: Ion chromatography anions results

www.manaraa.com

5.2 DOE Parameter Selection

5.2.1 Succinate Effectiveness Result

Figure 32 shows the current vs. time plot for 1000 ppm succinate ions. There was no short circuit during the time window studied. The current tended to decrease as time passed 180 seconds. There was no indication of dendrite growth after 180 seconds. This result showed that the effect of succinate on time to failure was insignificant. Thus, it was legitimate and reasonable to eliminate succinate off the DOE study.

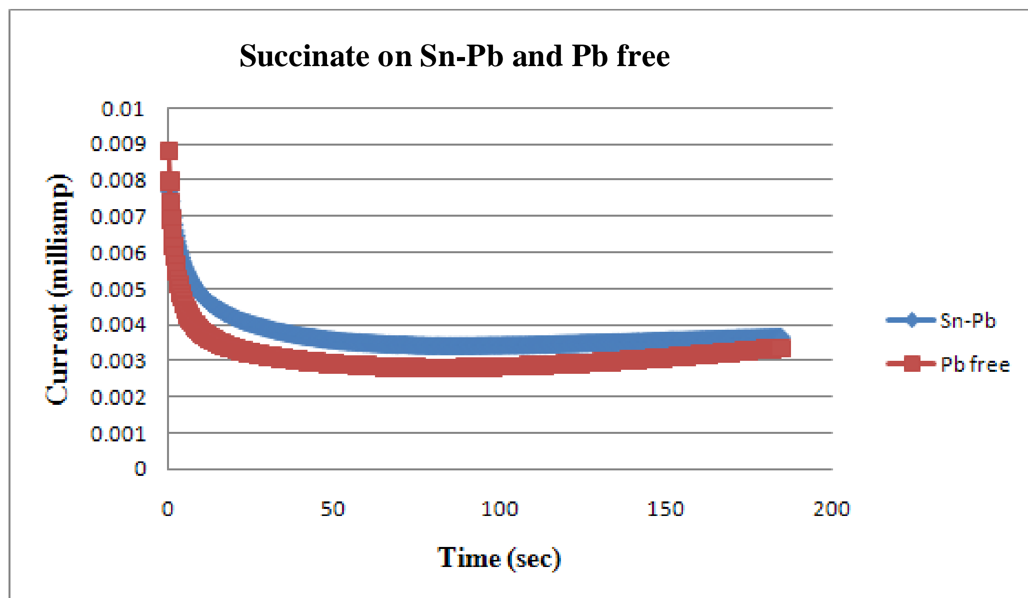

Figure 32: ECM plot (Current vs. Time) for 1000ppm succinate ions on tin-lead (Sn-Pb) and lead free (Pb free) boards

5.2.2 Final DOE Matrix

Because there was no significant effect of Succinate on time to failure, the final DOE matrix was revised for this study as in table 8. The final number of run for this study was 60. There was no organic acid anions in this study. There were only three anions: Chloride, Bromide, and Sulfate.

www.manaraa.com

Table 8: Final DOE matrix

Factors	Levels			Replicate	Responses
	1	2	3		
Anions	Cl^-	Br^-	SO^{4-}	5	Current and Time to Failure
Spacing	12.5	25			
Surface Finish	Tin Lead	Lead Free			

5.3 DOE Test Result

Response from each run was manually recorded on an individual basis. The result of sixty run DOE is shown below.

Table 9: DOE result

DOE PLAN						
Run	**Block**	**Parameters**			**Responses**	
		Anions	Surface finish	Spacing (mil)	Current (miliamp)	Time (sec.)
1	1	Cl_3ppm	Tin/Lead	12.5	0.1106933	22.52441
2	1	Cl_3ppm	Tin/Lead	25	2.798575	8.332031
3	1	Cl_3ppm	Lead free	12.5	0.1543589	6.791992
4	1	Cl_3ppm	Lead free	25	0.1310899	7.411133
5	1	Br_15ppm	Tin/Lead	12.5	0.1154548	28.65918
6	1	Br_15ppm	Tin/Lead	25	0.3042889	24.30273
7	1	Br_15ppm	Lead free	12.5	0.1105361	61.94727
8	1	Br_15ppm	Lead free	25	0.387433	25.82715
9	1	Sulfate_2ppm	Tin/Lead	12.5	1.041212	37.29004
10	1	Sulfate_2ppm	Tin/Lead	25	1.190811	15.4248
11	1	Sulfate_2ppm	Lead free	12.5	0.315529	162.9844
12	1	Sulfate_2ppm	Lead free	25	1.167376	32.6748
13	2	Cl_3ppm	Tin/Lead	12.5	0.1157627	32.67773
14	2	Cl_3ppm	Tin/Lead	25	2.169119	50.87402
15	2	Cl_3ppm	Lead free	12.5	0.1495795	5.864258
16	2	Cl_3ppm	Lead free	25	0.1143712	9.251953
17	2	Br_15ppm	Tin/Lead	12.5	0.5064873	55.49902
18	2	Br_15ppm	Tin/Lead	25	0.4082481	26.36816
19	2	Br_15ppm	Lead free	12.5	0.1049995	68.13086
20	2	Br_15ppm	Lead free	25	0.3213451	31.14258

المنارة للاستشارات
www.manaraa.com

Table 9: (continued)

21	2	Sulfate_2ppm	Tin/Lead	12.5	1.797316	58.26563
22	2	Sulfate_2ppm	Tin/Lead	25	1.091153	14.41016
23	2	Sulfate_2ppm	Lead free	12.5	0.7345902	41.63086
24	2	Sulfate_2ppm	Lead free	25	1.823513	43.14355
25	3	Cl_3ppm	Tin/Lead	12.5	0.1261358	15.41504
26	3	Cl_3ppm	Tin/Lead	25	1.975731	12.65137
27	3	Cl_3ppm	Lead free	12.5	0.1022478	9.87207
28	3	Cl_3ppm	Lead free	25	0.1406654	33.92285
29	3	Br_15ppm	Tin/Lead	12.5	0.1389758	34.84473
30	3	Br_15ppm	Tin/Lead	25	0.3961222	13.80859
31	3	Br_15ppm	Lead free	12.5	0.1011894	56.43652
32	3	Br_15ppm	Lead free	25	0.3018869	23.28711
33	3	Sulfate_2ppm	Tin/Lead	12.5	0.144669	42.8623
34	3	Sulfate_2ppm	Tin/Lead	25	2.584935	16.56445
35	3	Sulfate_2ppm	Lead free	12.5	0.1337577	108.5059
36	3	Sulfate_2ppm	Lead free	25	1.038044	47.67871
37	4	Cl_3ppm	Tin/Lead	12.5	0.1083965	32.98438
38	4	Cl_3ppm	Tin/Lead	25	2.074756	50.21777
39	4	Cl_3ppm	Lead free	12.5	0.1369792	4.623047
40	4	Cl_3ppm	Lead free	25	0.1449571	11.41602
41	4	Br_15ppm	Tin/Lead	12.5	0.1016564	24.37012
42	4	Br_15ppm	Tin/Lead	25	0.3257247	27.75781
43	4	Br_15ppm	Lead free	12.5	0.1295802	8.639648
44	4	Br_15ppm	Lead free	25	0.3090484	15.96387
45	4	Sulfate_2ppm	Tin/Lead	12.5	2.231781	79.84473
46	4	Sulfate_2ppm	Tin/Lead	25	1.367211	8.541016
47	4	Sulfate_2ppm	Lead free	12.5	0.3231619	120.0215
48	4	Sulfate_2ppm	Lead free	25	1.023792	44.61328
49	5	Cl_3ppm	Tin/Lead	12.5	0.128286	20.25391
50	5	Cl_3ppm	Tin/Lead	25	1.272251	24.04102
51	5	Cl_3ppm	Lead free	12.5	1.050266	7.702148
52	5	Cl_3ppm	Lead free	25	0.1465051	15.42676
53	5	Br_15ppm	Tin/Lead	12.5	0.1158731	41
54	5	Br_15ppm	Tin/Lead	25	0.3095593	63.07422
55	5	Br_15ppm	Lead free	12.5	0.1334971	17.58008
56	5	Br_15ppm	Lead free	25	0.3145386	39.37891
57	5	Sulfate_2ppm	Tin/Lead	12.5	1.585067	61.66016
58	5	Sulfate_2ppm	Tin/Lead	25	1.422541	14.80176

المنارة للاستشارات
www.manaraa.com

Table 9: (continued)

59	5	Sulfate_2ppm	Lead free	12.5	0.1943044	184.3555
60	5	Sulfate_2ppm	Lead free	25	1.084166	25.49316

Figure 33 is the test result of Cl^- 3 ppm on tin-lead board, spacing 12.5 mils. The short circuit clearly is defined for Chloride. Run number one shows that the current suddenly increased instantly up to 0.1106 milliamps and caused circuit short at 22.5 second. Furthermore, after 22.5 second the current decreased, this was because the flow of fluid or solution created by the applied voltage on the test cell was strong enough to break the ECM dendrite bridge between the pads. However, the current started increasing again and caused a circuit short. ECM kept growing and eventually appeared at anywhere between two pads.

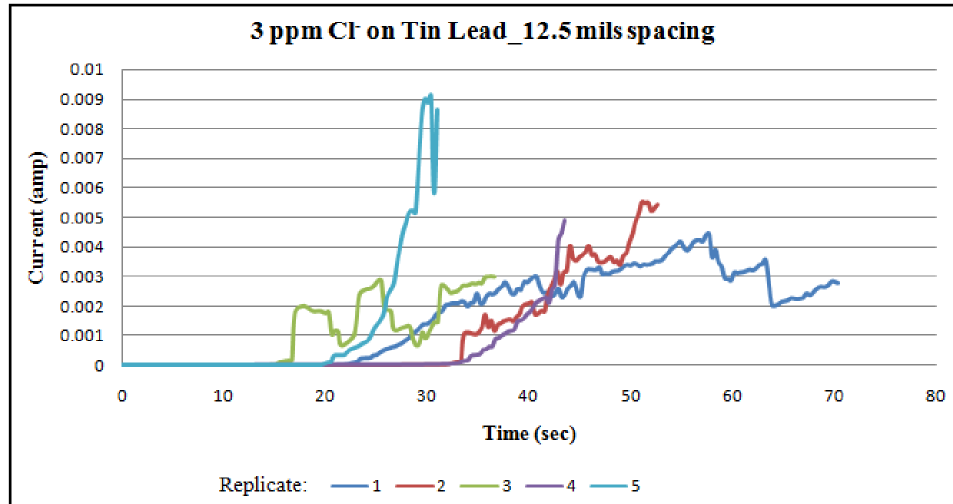

Figure 33: ECM plot (Current vs. Time) for 3 ppm Chloride anion on tin- lead 12.5 mils spacing

Figure 34 shows the short circuit in the tin-lead board, 25.0 mils spacing. The familiar pattern happened with 25.0 mils spacing. However, the time to failure range was

المنارة للاستشارات
www.manaraa.com

more abroad than the 12.5 mils. The time to failure for 12.5 mils was from 18 to 35 seconds while 25.0 mils spacing time to failure ranged from 9 to 60 seconds.

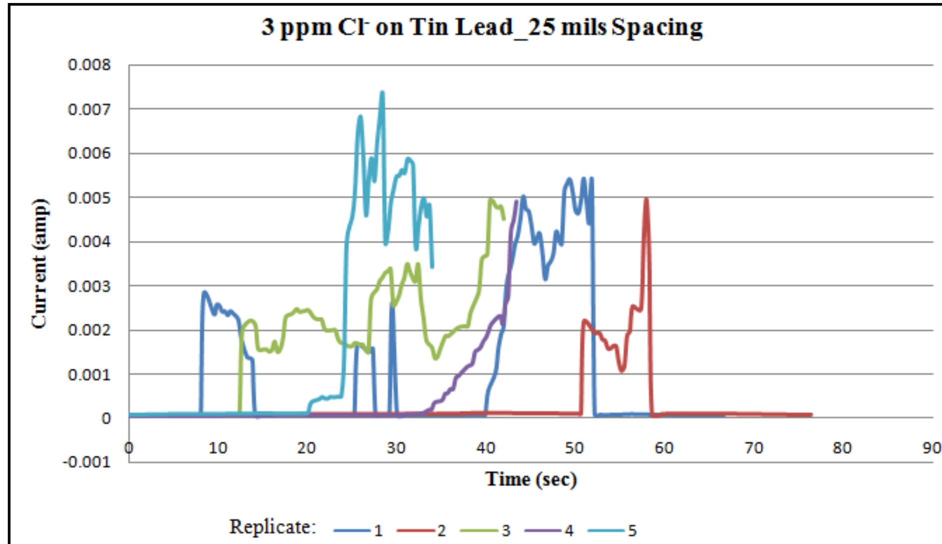

Figure 34: ECM plot (Current vs. Time) for 3 ppm Cl^- on tin lead_25.0 mils spacing

It was noticed that two different patterns of how the circuit short appeared. In figure 33 and 34, many test coupons started increasing steadily in current cause the circuit short(pattern 1). In contrast, many test coupons had current suddenly jumped up and cause circuit short (pattern 2). These two patterns repeated with other anions also and made it difficult to record the accurate response especially with pattern 1. Thus, to overcome this issue, each run was observed visually and recorded manually to know exactly when the circuit was short.

5.4 Effect of Pad Geometry and Field Strength on ECM Susceptibility

To estimate reliability risks due to ECM failures, the effect of different factors on time to failure was studied. Figure 35 shows the effect of aspect ratio on time to form dendritic shorts when 6.25V was applied across adjacent pads with different aspect ratios (the ratio of length over width of the pads, using a 3 ppm chloride solution. It is evident from this chart that failure occurs faster at larger aspect ratios.

المنارة للاستشارات
www.manaraa.com

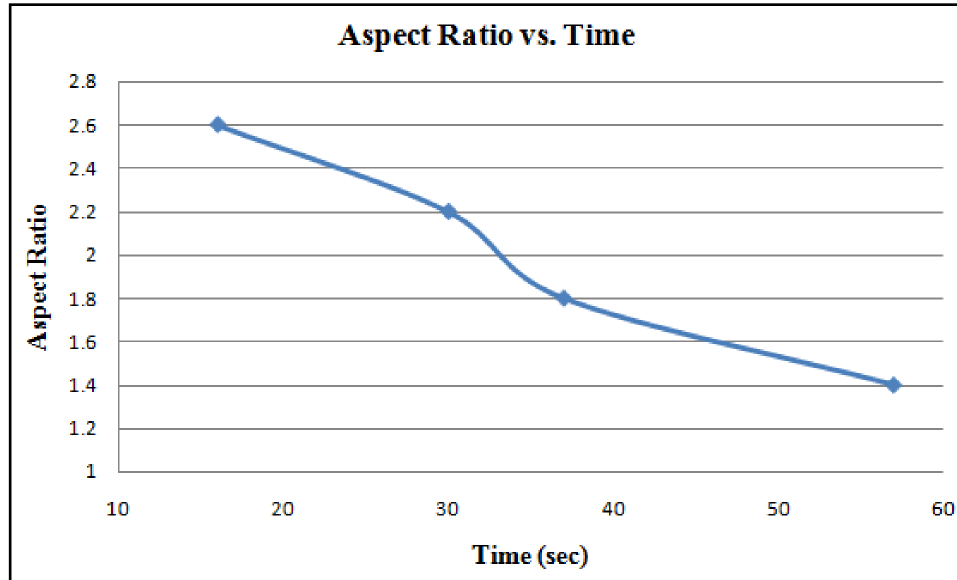

Figure 35: Aspect ratio vs. time

Figure 36 shows that current increases with increased spacing in tin-lead test board. Figure 37 shows a generally increasing trend in time to failure with increased spacing between electrodes in tin-lead test board. These two plots were obtained at a constant field strength of 0.5volt/mil.

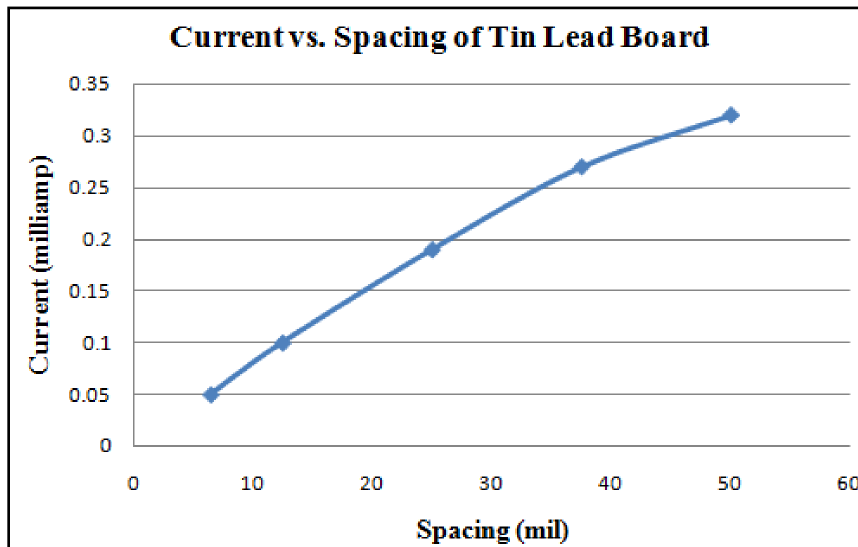

Figure 36: Current and spacing on tin lead board

المنارة للاستشارات
www.manaraa.com

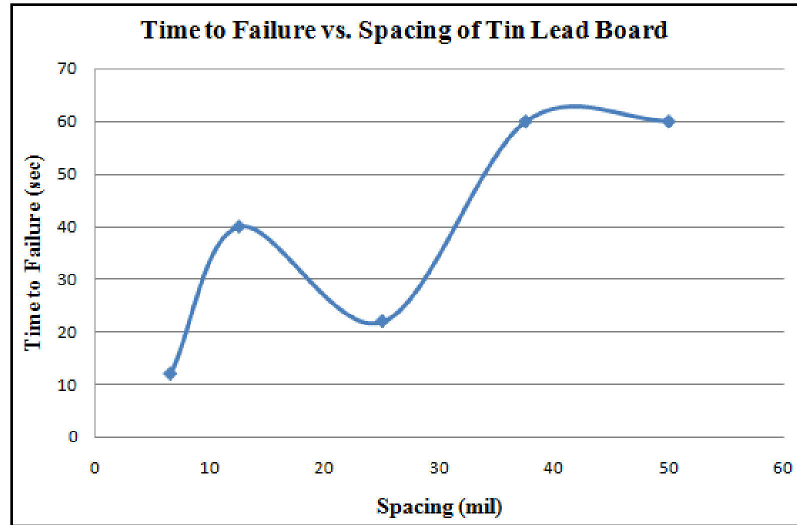

Figure 37: Time to failure vs. spacing on tin lead board

Figure 38 shows that WDT current on lead free board at the onset of dendritic shorts decreases dramatically as the spacing between the electrodes is increased from 6.25 to 50 mils. This is understandable because the field strength decreases with increased spacing. Figure 39 shows that time to failure on lead free has an increasing trend with spacing between the electrodes. This result indicates that the time to form shorts is related to the time for mass of tin dendrites to move across the two adjacent pads.

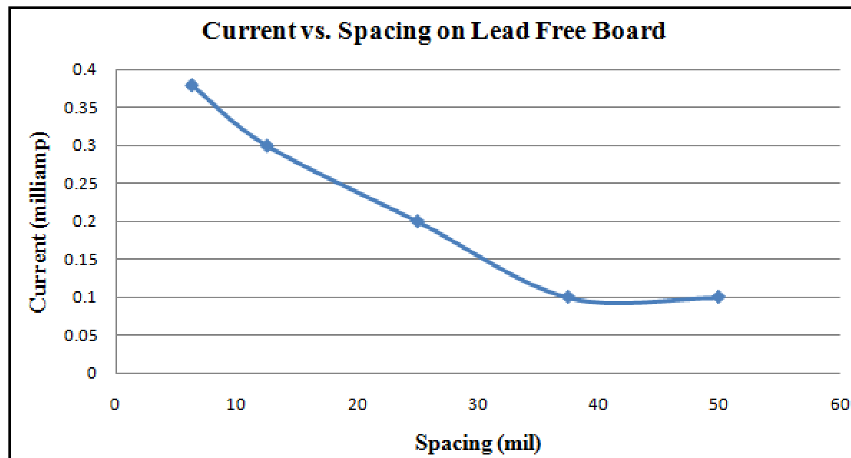

Figure 38: Current vs. spacing on lead free board

المنارة للاستشارات
www.manaraa.com

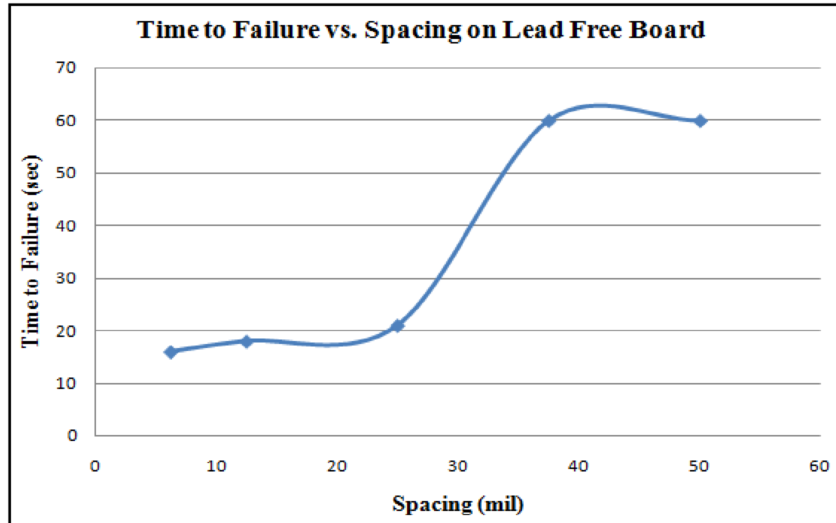

Figure 39: Time to failure vs. spacing on lead free board

5.5 Interaction Between Factors

Figure 40 presents trend plots that shows the influence of spacing, surface finish, and type of anion on time to failure.

In the anion-surface finish interaction plot, as the surface finish changes from Sn-Pb to Pb free, time to failure decreases in the presence of chloride, decreases in the presence of sulfate, and remains unchanged in the presence of bromide. This result indicates that the Pb free finish is more prone to dendrite formation than the Sn-Pb finish.

In the anion-spacing interaction trend plot, as the spacing increases from 12.5 mil to 25 mil, the time to failure decreases in the presence of sulfate and bromide, while it increases in the presence of chloride. At this point, it is not clear as to why the time to failure decreases with pad spacing in the presence of chloride ions.

In the surface finish-spacing interaction plot, it is evident that time to failure decreases with increased spacing for both of the surface finishes. This trend is not surprising since the dendritic growth is primarily a mass transfer process.

المنارة للاستشارات
www.manaraa.com

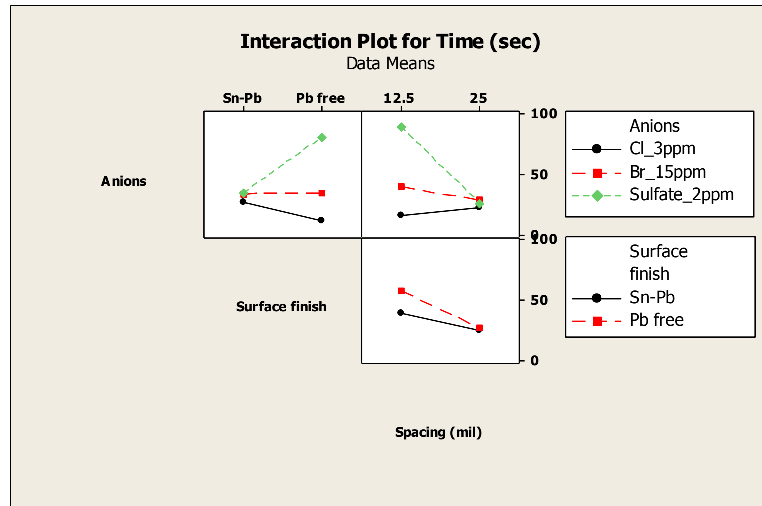

Figure 40: Interaction plot of factors for time (sec)

Figure 41 presents the influence of anion, surface finish, and spacing on current. In the anion-surface finish interaction plot, current decreases significantly as the surface finish changes from tin-lead to lead free for sulfate and chloride but remains mainly unchanged for bromide. In the anion-spacing interaction plot, it is seen that the current increases as the spacing increases for all three anions studied. In the surface finish-spacing interaction plot, the current increases with increased spacing for both surface finishes.

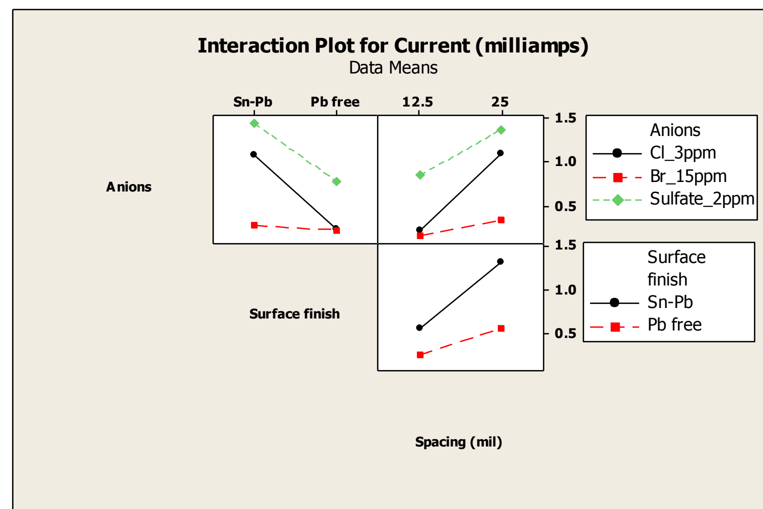

Figure 41: Interaction plot of factors for current (milliamps)

المنارة للاستشارات
www.manaraa.com

5.6 Statistical Analysis

The statistical analysis was performed to evaluate the significance of data. The probability of making a type error sigma σ is 0.05. To determine the effect of variances on time to failure and current, P-value is compared with σ level. If P-value is less than 0.05, the effect of variance is significant and vise versa.

Figure 42 shows the P-value of interaction between anions, surface finish and spacing is greater than 0.05. This interaction does not have a significant effect on time to failure. Similarly, the interaction between surface finish and spacing is also insignificant. On the other hand, the interaction between anions versus surface finish and anions versus spacing effects significantly on time to failure result. Regarding individual variance, surface finish has no significant effect on time to failure, as well as blocks. In this experiment, block is defined by running test coupon on different days. In contrast, anions and spacing are two significant variances that effect mostly on time to failure result.

Analysis of Variance for Time (sec), using Adjusted SS for Tests

Source	DF	Seq SS	Adj SS	Adj MS	F	P
Blocks	4	512.0	512.0	128.0	0.27	0.896
Anions	2	15384.4	15384.4	7692.2	16.22	0.000
Surface finish	1	1626.5	1626.5	1626.5	3.43	0.071
Spacing (mil)	1	7603.6	7603.6	7603.6	16.03	0.000
Anions*Surface finish	2	10266.7	10266.7	5133.3	10.82	0.000
Anions*Spacing (mil)	2	13273.1	13273.1	6636.5	13.99	0.000
Surface finish*Spacing (mil)	1	971.8	971.8	971.8	2.05	0.159
Anions*Surface finish*Spacing (mil)	2	1448.1	1448.1	724.0	1.53	0.229
Error	44	20867.4	20867.4	474.3		
Total	59	71953.5				

Figure 42: Data analysis of variances on time to failure

Figure 43 shows the interaction between variances and individual variance has significant effects on the current result. While block variance shows no significant effect

المنارة للاستشارات
www.manaraa.com

on current.

Analysis of Variance for Current (milli amps), using Adjusted SS for Tests

Source	DF	Seq SS	Adj SS	Adj MS	F	P
Blocks	4	0.2157	0.2157	0.0539	0.37	0.832
Anions	2	7.5401	7.5401	3.7701	25.54	0.000
Surface finish	1	4.1268	4.1268	4.1268	27.96	0.000
Spacing (mil)	1	4.2121	4.2121	4.2121	28.54	0.000
Anions*Surface finish	2	1.7818	1.7818	0.8909	6.04	0.005
Anions*Spacing (mil)	2	1.2129	1.2129	0.6065	4.11	0.023
Surface finish*Spacing (mil)	1	0.7592	0.7592	0.7592	5.14	0.028
Anions*Surface finish*Spacing (mil)	2	5.5215	5.5215	2.7607	18.70	0.000
Error	44	6.4945	6.4945	0.1476		
Total	59	31.8646				

Figure 43: Data analysis of variances on current

Figure 44 presents a box plot of time to failure as a function of spacing, surface finish, and anion For chloride, the lead free finish fails slightly faster than the tin-lead finish. For bromide: the difference between tin-lead and lead free is statistically insignificant. For sulfate, the 25 mils spacing fails faster than the 12.5 mils spacing.

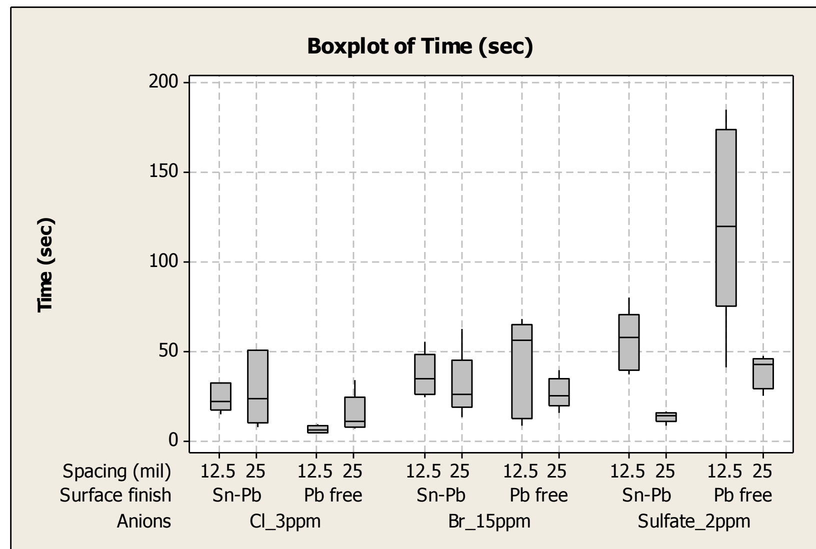

Figure 44: Variables vs. time to failure (sec)

Figure 45 presents the box plot of current at failure as a function of spacing, surface finish, and anion.

المنارة للاستشارات
www.manaraa.com

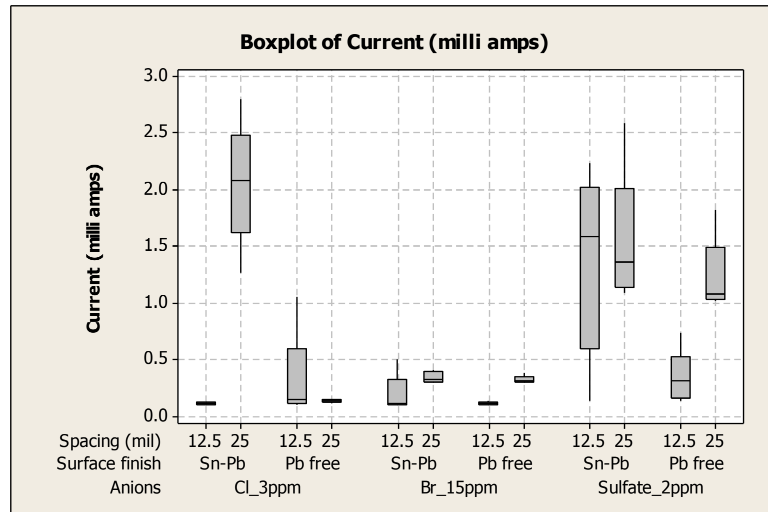

Figure 45: Variables vs. current at failure (milliamps)

For chloride, Pb free appears to show least variation in the current with the two spacings while Sn-Pb shows a large difference in the current to failure between the two spacings. For bromide, there is an exceptionally small variability in the current at failure between the two surface finishes and there is a slight difference in the WDT current at failure with different pad spacings. For sulfate, average median WDT current at failure is lower for Pb free than Sn-Pb.

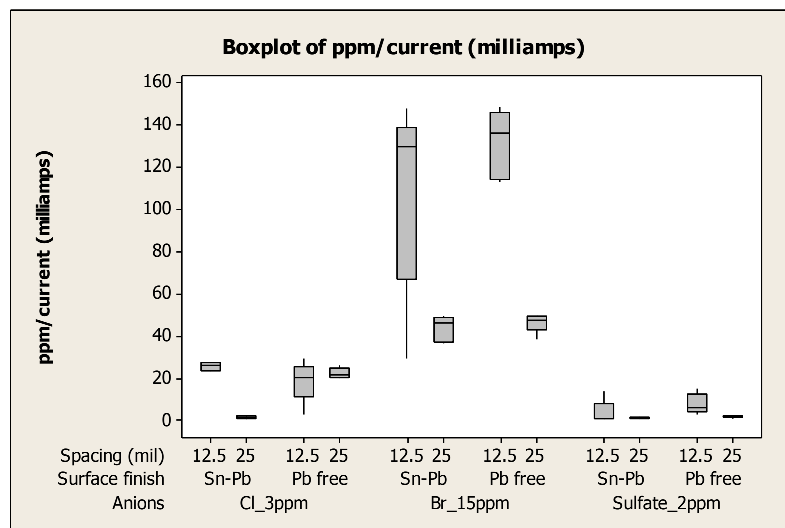

Figure 46: Total anions (ppm) over WDT current vs. test variables

المنارة للاستشارات
www.manaraa.com

In order to compare the effect of different anions, we normalized the ppm levels of anions by plotting the ratios of anion ppm per WDT current and anion ppm per unit time as a function of the various test variables. Figure 46 shows that sulfate concentration required to cause dendritic failures is the lowest per unit WDT current. Bromide exhibits the highest ppm levels per unit WDT current with chloride being slightly higher than sulfate.

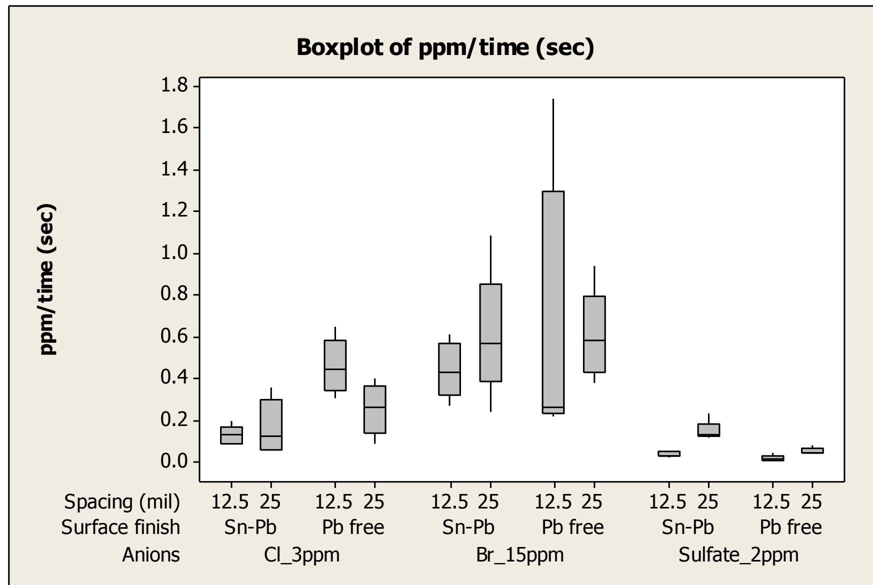

Figure 47: Ppm over time vs. test variables

Figure 47 shows that sulfate again exhibits the lowest ppm levels per unit time to failure while bromide required the highest concentration to cause failure per unit time. The ppm level of chloride that causes failures is only slightly higher than sulfate.

المنارة للاستشارات
www.manaraa.com

CHAPTER 6: CONCLUSION AND FUTURE WORK

6.1 Conclusion

In this thesis, the study of time to cause the failures was presented. A test vehicle was developed for the WDT to obtain the time to cause ECM failure in presence of different anions. Based on the results, the activity of each anions was the main effect on time to failure. The water drop test could be used to assess the propensity of various anions to form dendrites. Pad geometry and spacing had significant effects on dendritic growth. The threshold ppm level of sulfate required to cause dendritic failure was the lowest among the various anions tested. While the threshold ppm level of bromide required to cause dendritic failure was the highest among the various anions tested. Succinate ions failed to cause any dendritic growth at 1000 ppm concentration.

6.2 Future Work

Based on the power law, there's a chance the data acquired in this study can lead to the default or wrong lead because of the unknown variance that may affect the result in this study. In order to meaningfully apply this technique to real field conditions, more experiments need to be performed. It is suggested evaluating this test by applying several monolayers of water containing known concentrations of anions as well as evaluating mixtures of various anions, including other weak organic acids. Furthermore, more inorganic acid such as nitrate, fluoride and phosphate are also suggested evaluating.

المنارة للاستشارات
www.manaraa.com

On the other hand, even though cleaning the "as received" boards eliminated the some of the contamination, the percentage of metals on the boards are still unknown. Thus, evaluating the percentage amount of tin, lead, and copper or any metals present on the test sample is beneficial to determine time to failure. Gold nanoparticles will be a powerful solution combining with cyclic voltametry (figure 48 and 49) technique to detect the concentration of metals such as tin, lead, copper, zinc on the as received boards so that time to failure results will be accurate with fewer variances.

Below is a picture of gold nanoparticles successfully created and characterized under TEM (Transmitted Electron Microscopy) equipment.

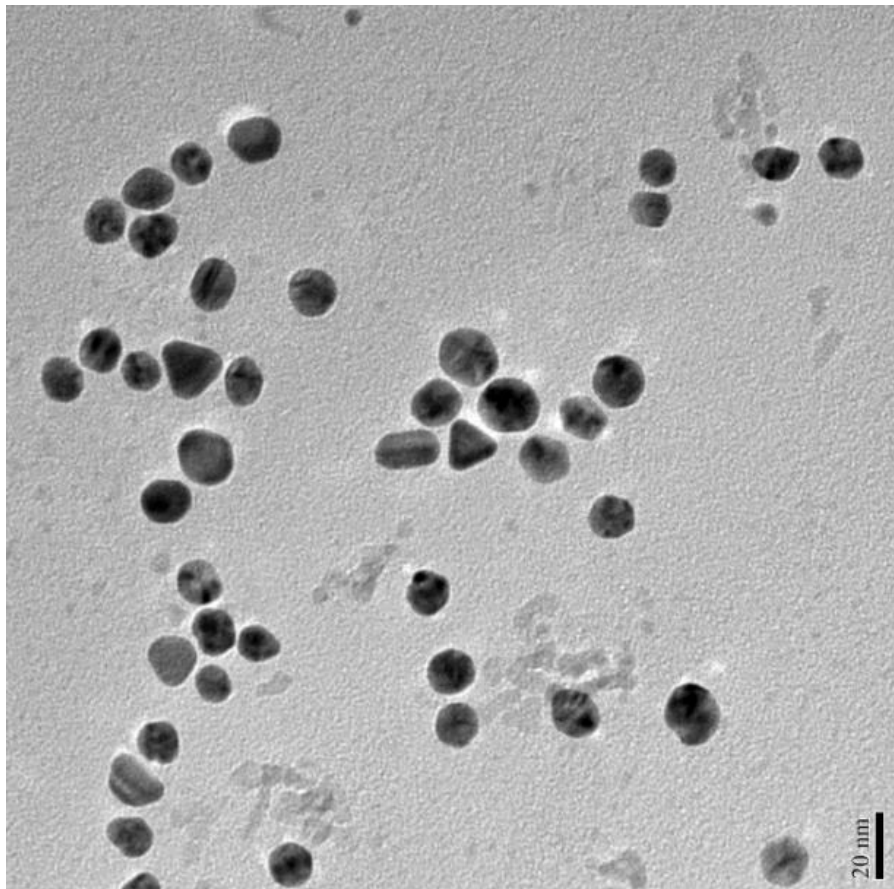

Figure 48: Gold nanoparticles under TEM x 20 nm.

المنارة للاستشارات
www.manaraa.com

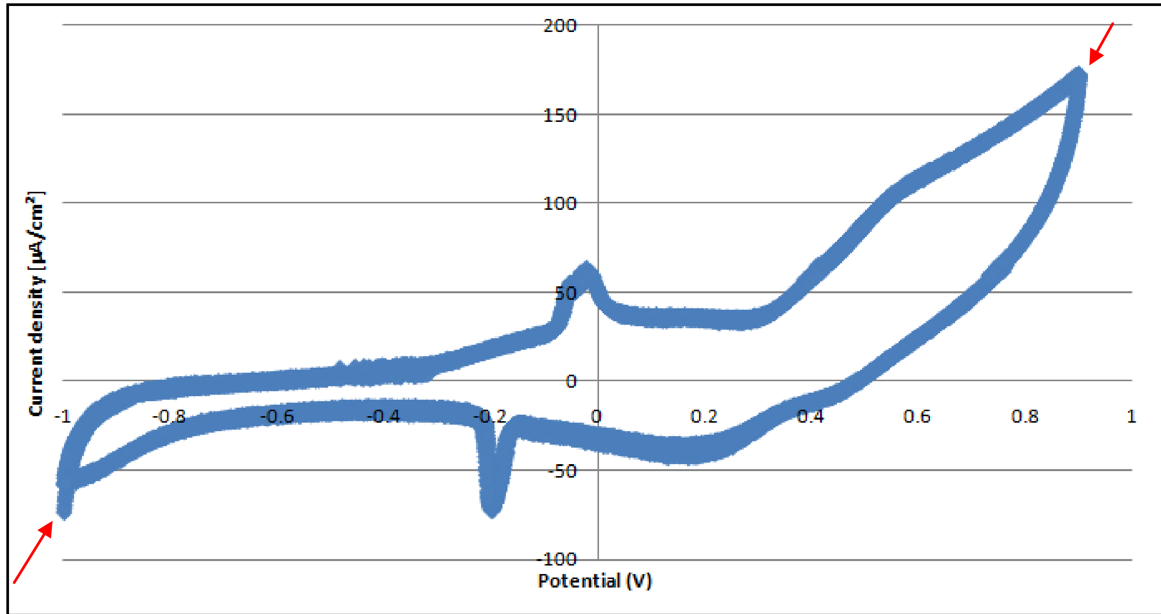

Figure 49: Potential vs. current density of Zn^{2+} in gold nanoparticles solution

Figure 49 shows the cyclic Voltametry system detects Zn^{2+} by identify the potential of Zn^{2+} which is +/-0.73.

المنارة للاستشارات
www.manaraa.com

REFERENCES

B. Engel, E. Levine, J. Petrus, and A. Shore. (2004). The Art of Cross Sectioning. In *Microelectronics Failure Analysis* (5th Edition ed., p. 481). ASM.

Brian A. Smith and Laura J. Turbini. (1999). Characterizing the Weak Organic Acids Used in Low Solids Fluxes. *Electronic Materials , 28* (11).

Bruckner, M. (n.d.). *Microbial Life Educational Resources*. Retrieved 09 24, 2012, from http://serc.carleton.edu/microbelife/research_methods/biogeochemical/ic.html

Capillo, C. (1990). *Surface Mount Technology.* New York: McGraw-Hill.

Csaba Dominkovics, Gabor Harsanyi. (2008). Farctal description of dendrite growth during electrochemical migration. *Microelectronics Reliability , 48*, 1628-1634.

D.Q. Yu et al. (2006). Electrochemical migration of Sn-Pb and lead free solder alloys under distilled water. *Matter Electron* , 219-227.

Deckert, C. (1987). Quality and Productivity Advances in Plated Through-Hole Technology. *Printed Circuit World Convetion IV.*

Doss, K. (2011). *Soldering Paste 101.* Jabil.

E. Bimiller and C. Hillman. (2004). The Effect of Electric Field and Halide Contamination on Electrochemical Migration. *SMTA Pan Pac.*

Eith, C. (2001). Practical Ion Chromatography. Metrohm Ltd.

Ellis, N. B. (1986). *Cleaning and Contamination of Electronics Components and Assemblies.*

Foresite. (n.d.). *Forsite*. Retrieved 11 06, 2012, from A Localized Cleanliness Tester and Extraction System: http://www.residues.com/C3.html

Harsanyi. (1999). Copper may destroy chip-level reliability: Handle with care mechanism and conditions for copper migrated resistive short formation. *IEEE Electron Device Letters*, *20*, pp. 5-8.

Harsanyi, G. (1995). Electrochemical Processes Resulting in Migrated Short Failures in Microcircuits. *IEEE , 18* (3).

المنارة للاستشارات
www.manaraa.com

Harsanyi, G. (1995). Electrochemical Processes Resulting in Migrated Short Failures in Microcircuits. *IEEE Transactions on Components Packaging and Manufacturing Technology*, *18*, pp. 602-610.

Hilman, C. (2010). Contamination and Cleanliness: Developing Practical Responses to a Challenging Problem. *SMTA International*, (p. 7). Orlando.

Hornung, A. (1968). Diffusion of silver in borosilicate glass. *Electronics Components Conference* (pp. 250-5). New York: USE: IEEE.

Hwang, S. J. (1992). *Solder Paste in Electronics Packaging: Technology and Applications in Surface Mount, Hybrid Circuits, and Component Assembly.*

Hymes, L. (1991). *Cleaning Printed Wiring Assemblies in Today's Environment.* New York: Van Nosrand Reinhold.

IPC. (1997). *Electrochemical Migration: Electrically induced Failures in Printed Wiring Assemblies".* Northbrook, IL: IPC-TR476A.

J. Barton and J. Bockris. (1962). The electrolytic growth of dendrites from ionic solutions. *Royal Society of London Proceedings*, (pp. 485-505).

Kong Hui Lee, Rob Jukna, Jim Altpeter, Kantesh Doss. (2011). Comparision of ROSE, C3/IC, and SIR as an effective cleanliness verification test for post soldered PCBA. *Soldering & Surface Mount Technology , 23* (2).

L. Zou and C. Hint. (1999). *The Effect of Test Voltage, Test Pattern and Board Finish on Surface Insulation Resistance Measurements for Various Fluxes.* NPL Report CMMTA (A) 222.

Lawson, W. (2007). *The Effects of Design and Environmental Factos on The Reliability of Elctronic Products.* University of Slaford.

Murarka Shyam P., Verner Igor V., and Gutmann Ronald J. (2000). *Copper-Fundamental Mechanisms for Mircroelectronic Applications.*

Muren, D. (1994). Atmosphere Influence on Relfow Soldering. *AGA* .

Noh et al. (2008). Behaviour of electrochemical migration with solder alloys on printed circuit boards (PCBs). *Circuit World* .

O. Devos, C. Gabrielli, L. Beitone, C. Mace, E. Ostemann, H. Perrot. (2007). Growth of electrolytic copper dendrites. II: Oxalic acid medium. *Electroanalytical Chemistry*

.

المنارة للاستشارات

www.manaraa.com

O. Devos, C. Gabrielli, L. Beitone, C. Mace, E. Ostermann, H. Perrot. (2007). Growth of elctrolytic copper dendrites. I: Current transients and optical observation. *Electroanalytical Chemistry* .

Pravin Sequeira et al. (2010). Ion Contamination Assessment. *SMTAI 2010.* Orlando.

Ready, W. J and Turnini, L. J. (2002). The effect of flux chemistry, applied voltage, conductor spacing, and temperature on coductive anodic filament formation. *Journal of Electronic Materials* , 1208-1224.

Shangguan D., Achari A. and Green W. (1994). Application of lead-free eutectic Sn-Ag solder in no-clean thick film electronic modules. *Advanced Pacaging. 17*, pp. 603-611. IEEE.

Sheng Zhan, Micheal H. Azarian, and Micheal G. Pecht. (2006). Surface Insulation Resistance of Confromally Coated Printed Circuit Boards Processed With No-Clean Flux. *IEEE , 29* (3).

Siliconfareast. (n.d.). Retrieved 09 17, 2012, from Siliconfareast : http://www.siliconfareast.com/sectioning.htm

Stearns, T. H. (1996). *Flexible Prited Circuitry.* New York: McGraw-Hill.

Strauss, R. (1994). *Surface Mount Technology.* Oxford: Butterworth-Heinemann.

W. Jud Ready, Laura J. Turbini, Roger Nickel, and John Fischer. (1999). A Novel Test Circuit for Automatically Detecting Electrochemical Migration and Conductive Anodic Filament Formation. *Electronic Materials , 28* (No. 11).

المنارة للاستشارات
www.manaraa.com

APPENDICES

المنارة للاستشارات
www.manaraa.com

Appendix A: Collected Data for Ion Chromatography

This is a cleaning process result for Bag Extraction in DI water.

Bag Blank

Anion	ug/ml	Total ug
Fluoride		0.00
Chloride	0.024	0.72
Bromide		0.00
Nitrite		0.00
Nitrate	0.04	1.20
Sulfate	0.013	0.39
Phosphate	0.006	0.18
Acetate	0.052	1.56
MSA	0.554	16.62
Succinate	0.004	0.12
Total WOA	0.61	18.30
Total Inorganic anions	0.08	2.49
TOTAL	0.69	20.79

LE11_in 30ml DI

Anion	ug/ml	Total ug	ug/in.sq.
Fluoride	0.007	0.21	0.01
Chloride	0.124	3.00	0.10
Bromide	6.843	205.29	6.84
Nitrite	0.002	0.06	0.00
Nitrate	0.080	1.20	0.04
Sulfate	0.047	1.02	0.03
Phosphate		-0.18	-0.01
Acetate	0.123	2.13	0.07
MSA	2.375	54.63	1.82
Succinate	0.030	0.78	0.03
Total WOA	2.53	57.54	1.92
Total Inorganic anions	7.10	210.60	7.02
TOTAL	9.63	268.14	8.94

المنارة للاستشارات
www.manaraa.com

Appendix A (continued)

LE05_in 1/10 (30ml)

Anion	ug/ml	Total ug	ug/in.sq.
Fluoride	0.002	0.06	0.02
Chloride	0.029	0.15	0.05
Bromide	0.152	4.56	1.52
Nitrite		0.00	0.00
Nitrate	0.267	6.81	2.27
Sulfate	0.140	3.81	1.27
Phosphate	0.009	0.09	0.03
Acetate	0.736	20.52	6.84
MSA	1.269	21.45	7.15
Succinate	0.001	-0.09	-0.03
Total WOA	2.01	41.88	13.96
Total Inorganic anions	0.60	15.48	5.16
TOTAL	2.61	57.36	19.12

This is a cleaning process result for Bag Extraction in IPA

Bag Blank

Anion	ug/ml	Total ug
Fluoride	0	0.00
Chloride	0.043	1.29
Bromide	0	0.00
Nitrite	0	0.00
Nitrate	0.244	7.32
Sulfate	0.009	0.27
Phosphate	0	0.00
Acetate	0.118	3.54
MSA	0.841	25.23
Succinate	0.005	3 0.15
4 Total WOA	5 0.96	6 28.92
7 Total Inorganic anions	8 0.30	9 8.88
10 TOTAL	11 1.26	12 37.80

المنارة للاستشارات
www.manaraa.com

Appendix A (continued)

LE21_in 30ml IPA/DI

Anion	ug/ml	Total ug	ug/in.sq.
Fluoride	0	0.00	0.00
Chloride	0.225	5.46	0.18
Bromide	7.889	236.67	7.89
Nitrite	0.000	0.00	0.00
Nitrate	0.634	11.70	0.39
Sulfate	0.030	0.63	0.02
Phosphate	0.027	0.81	0.03
Acetate	1.006	26.64	0.89
MSA	3.952	93.33	3.11
Succinate	0.030	0.75	0.03
Total WOA	4.99	120.72	4.02
Total Inorganic anions	8.81	255.27	8.51
TOTAL	13.79	375.99	12.53

LE07_in 30ml IPA/DI

Anion	ug/ml	Total ug	ug/in.sq.
Fluoride	0	0.00	0.00
Chloride	0.302	7.77	0.26
Bromide	1.887	56.61	1.89
Nitrite	0.000	0.00	0.00
Nitrate	2.125	56.43	1.88
Sulfate	0.350	10.23	0.34
Phosphate	0.000	0.00	0.00
Acetate	12.720	378.06	12.60
MSA	13.158	369.51	12.32
Succinate	0.000	-0.15	-0.01
Total WOA	25.88	747.42	24.91
Total Inorganic anions	4.66	131.04	4.37
TOTAL	30.54	878.46	29.28

المنارة للاستشارات
www.manaraa.com

Appendix A (continued)

This is the cleaning process result for C3 extraction in DI water.

LE11_G			
Anion	ug/ml	Total ug	ug/in.sq.
Fluoride	0.004	0.010	0.096
Acetate	0.017	0.041	0.408
MSA (or formate)	0.259	0.622	6.216
Chloride	0.035	0.084	0.840
Bromide	0.218	0.523	5.232
Nitrite	0.002	0.005	0.048
Nitrate	0.009	0.022	0.216
Sulfate	0.082	0.197	1.968
Phosphate	0.012	0.029	0.288
Succinate	0.039	0.094	0.936
Total WOA	0.315	0.756	7.560
Total Inorganic anions	0.362	0.869	8.688
TOTAL	0.677	1.625	16.248

LE11_H			
Anion	ug/ml	Total ug	ug/in.sq.
Fluoride	0.004	0.010	0.096
Acetate	0.016	0.038	0.384
MSA (or formate)	0.267	0.641	6.408
Chloride	0.041	0.098	0.984
Bromide	0.261	0.626	6.264
Nitrite	0.001	0.002	0.024
Nitrate	0.009	0.022	0.216
Sulfate	0.096	0.230	2.304
Phosphate	0.005	0.012	0.120
Succinate	0.022	0.053	0.528
Total WOA	0.305	0.732	7.320
Total Inorganic anions	0.417	1.001	10.008
TOTAL	0.722	1.733	17.328

المنارة للاستشارات
www.manaraa.com

Appendix A (continued)

LE21_G

Anion	ug/ml	Total ug	ug/in.sq.
Fluoride	0.006	0.014	0.144
Acetate	0.010	0.024	0.240
MSA (or formate)	0.226	0.542	5.424
Chloride	0.088	0.211	2.112
Bromide	0.276	0.662	6.624
Nitrite	0.002	0.005	0.048
Nitrate	0.011	0.026	0.264
Sulfate	0.087	0.209	2.088
Phosphate	0.015	0.036	0.360
Succinate	0.087	0.209	2.088
Total WOA	0.323	0.775	7.752
Total Inorganic anions	0.485	1.164	11.640
TOTAL	0.808	1.939	19.392

LE21_H

Anion	ug/ml	Total ug	ug/in.sq.
Fluoride	0.004	0.010	0.096
Acetate	0.017	0.041	0.408
MSA (or formate)	0.257	0.617	6.168
Chloride	0.038	0.091	0.912
Bromide	0.301	0.722	7.224
Nitrite	0.002	0.005	0.048
Nitrate	0.006	0.014	0.144
Sulfate	0.109	0.262	2.616
Phosphate	0.008	0.019	0.192
Succinate	0.022	0.053	0.528
Total WOA	0.296	0.710	7.104
Total Inorganic anions	0.468	1.123	11.232
TOTAL	0.764	1.834	18.336

المنارة للاستشارات
www.manaraa.com

Appendix A (continued)

This is the cleaning process result for C3 extraction in IPA.

LE05_G			
Anion	ug/ml	Total ug	ug/in.sq.
Fluoride	0.005	0.012	0.120
Acetate	0.261	0.626	6.264
MSA (or formate)	1.226	2.942	29.424
Chloride	0.058	0.139	1.392
Bromide	0.008	0.019	0.192
Nitrite	0.002	0.005	0.048
Nitrate	0.236	0.566	5.664
Sulfate	0.231	0.554	5.544
Phosphate	0.014	0.034	0.336
Succinate	0.022	0.053	0.528
Total WOA	1.509	3.622	36.216
Total Inorganic anions	0.554	1.330	13.296
TOTAL	2.063	4.951	49.512

LE05_H			
Anion	ug/ml	Total ug	13 ug/in.sq.
14 Fluoride	15 0.005	16 0.012	17 0.120
18 Acetate	19 0.316	20 0.758	21 7.584
22 MSA (or formate)	23 1.496	24 3.590	25 35.904
26 Chloride	27 0.055	28 0.132	29 1.320
30 Bromide	31 0.009	32 0.022	33 0.216
34 Nitrite	35 0.003	36 0.007	37 0.072
38 Nitrate	39 0.253	40 0.607	41 6.072
42 Sulfate	43 0.290	44 0.696	45 6.960
46 Phosphate	47 0.013	48 0.031	49 0.312
50 Succinate	51 0.044	52 0.106	53 1.056
54 Total WOA	55 1.856	56 4.454	57 44.544
58 Total Inorganic anions	59 0.628	60 1.507	61 15.072
62 TOTAL	63 2.484	64 5.962	65 59.616

للاستشارات المنارة
www.manaraa.com

Appendix A (continued)

LE14_G

Anion	ug/ml	Total ug	ug/in.sq.
Fluoride	0.008	0.019	0.192
Acetate	0.267	0.641	6.408
MSA (or formate)	1.585	3.804	38.040
Chloride	0.068	0.163	1.632
Bromide	0.012	0.029	0.288
Nitrite	0.002	0.005	0.048
Nitrate	0.148	0.355	3.552
Sulfate	0.281	0.674	6.744
Phosphate	0.010	0.024	0.240
Succinate	0.024	0.058	0.576
Total WOA	1.876	4.502	45.024
Total Inorganic anions	0.529	1.270	12.696
TOTAL	2.405	5.772	57.720

LE14_H

Anion	ug/ml	Total ug	ug/in.sq.
Fluoride	0.007	0.017	0.168
Acetate	0.276	0.662	6.624
MSA (or formate)	2.017	4.841	48.408
Chloride	0.077	0.185	1.848
Bromide	0.008	0.019	0.192
Nitrite		0.000	0.000
Nitrate	0.516	1.238	12.384
Sulfate	0.364	0.874	8.736
Phosphate	0.006	0.014	0.144
Succinate		0.000	0.000
Total WOA	2.293	5.503	55.032
Total Inorganic anions	0.978	2.347	23.472
TOTAL	3.271	7.850	78.504

www.manaraa.com

Appendix B: Collected Data for Conductivity Test

Below is the conductivity test result in DI Water.

Concentration (ppm)	Chloride	Bromide	Sulfate	Succinate
1	3.8	1.1	2.3	0.7
4	16.2	7.0	12.7	5.9
10	42.6	19.3	32.1	14.8
50	223	99.1	163	87.4
100	447	210	329	177.0
1000			2940	

Below is the conductivity test result in IPA.

Concentration (ppm)	Chloride	Bromide	Sulfate	Succinate
1	0	0	0	N/A
4	2.2	0	2.8	0
10	7.3	2.6	4.6	2.0
50	41.4	21.6	24.9	20.1
100	85.2	46.8	51.3	40.2

www.manaraa.com

Appendix C: Permission Release for Use of Result from Work at Jabil Inc.

10/05/2012

Letter of Permission

The information that I have collected from Jabil Inc. is fully accurate and legitimate. I, Minh Nguyen, ask Jabil's permission to use the information in my thesis paper: "Reliability Assessment of Ion Contamination Residues in Printed Circuit Board" for my thesis defense in accordance to meet the requirement of University of South Florida copyright.

Requester	Title	Date
Minh Nguyen	USF Student	10/05/2012

Name	Title	Date
ARTHUR G. RAWERS	MANAGER, GLOBAL FAILURE ANALYSIS	10/05/2012

للاستشارات المنارة

www.manaraa.com